NATIONAL ADVISORY COMMITTEE FOR AERONAUTICS

REPORT No. 682

FLAME SPEEDS AND ENERGY CONSIDERATIONS FOR EXPLOSIONS IN A SPHERICAL BOMB

By ERNEST F. FIOCK, CHARLES F. MARVIN, Jr.
FRANK R. CALDWELL, and CARL H. ROEDER

1940

For sale by the Superintendent of Documents, Washington, D. C. - - - - - - - - - - - - - - - - Price 10 cents
Subscription price, $3 per year

AERONAUTIC SYMBOLS

1. FUNDAMENTAL AND DERIVED UNITS

	Symbol	Metric		English	
		Unit	Abbreviation	Unit	Abbreviation
Length	l	meter	m	foot (or mile)	ft. (or mi.)
Time	t	second	s	second (or hour)	sec. (or hr.)
Force	F	weight of 1 kilogram	kg	weight of 1 pound	lb.
Power	P	horsepower (metric)		horsepower	hp.
Speed	V	kilometers per hour	k.p.h.	miles per hour	m.p.h.
		meters per second	m.p.s.	feet per second	f.p.s.

2. GENERAL SYMBOLS

W, Weight $=mg$

g, Standard acceleration of gravity $=9.80665$ m/s^2 or 32.1740 ft./sec.^{2}

m, Mass $=\frac{W}{g}$

I, Moment of inertia $=mk^2$. (Indicate axis of radius of gyration k by proper subscript.)

μ, Coefficient of viscosity

ν, Kinematic viscosity

ρ, Density (mass per unit volume)

Standard density of dry air, 0.12497 kg-m^{-4}-s^2 at 15° C. and 760 mm; or 0.002378 lb.-ft.$^{-4}$ sec.^{2}

Specific weight of "standard" air, 1.2255 kg/m^3 or 0.07651 lb./cu. ft.

3. AERODYNAMIC SYMBOLS

S, Area

S_w, Area of wing

G, Gap

b, Span

c, Chord

$\frac{b^2}{S}$, Aspect ratio

V, True air speed

q, Dynamic pressure $=\frac{1}{2}\rho V^2$

L, Lift, absolute coefficient $C_L=\frac{L}{qS}$

D, Drag, absolute coefficient $C_D=\frac{D}{qS}$

D_0, Profile drag, absolute coefficient $C_{D_0}=\frac{D_0}{qS}$

D_i, Induced drag, absolute coefficient $C_{D_i}=\frac{D_i}{qS}$

D_p, Parasite drag, absolute coefficient $C_{D_p}=\frac{D_p}{qS}$

C, Cross-wind force, absolute coefficient $C_C=\frac{C}{qS}$

R, Resultant force

i_w, Angle of setting of wings (relative to thrust line)

i_t, Angle of stabilizer setting (relative to thrust line)

Q, Resultant moment

Ω, Resultant angular velocity

$\rho\frac{Vl}{\mu}$, Reynolds Number, where l is a linear dimension (e.g., for a model airfoil 3 in. chord, 100 m.p.h. normal pressure at 15° C., the corresponding number is 234,000; or for a model of 10 cm chord, 40 m.p.s., the corresponding number is 274,000)

C_p, Center-of-pressure coefficient (ratio of distance of c.p. from leading edge to chord length)

α, Angle of attack

ϵ, Angle of downwash

α_0, Angle of attack, infinite aspect ratio

α_i, Angle of attack, induced

α_a, Angle of attack, absolute (measured from zero-lift position)

γ, Flight-path angle

REPORT No. 682

FLAME SPEEDS AND ENERGY CONSIDERATIONS FOR EXPLOSIONS IN A SPHERICAL BOMB

By ERNEST F. FIOCK, CHARLES F. MARVIN, Jr.
FRANK R. CALDWELL, and CARL H. ROEDER

National Bureau of Standards

NATIONAL ADVISORY COMMITTEE FOR AERONAUTICS

HEADQUARTERS, NAVY BUILDING, WASHINGTON, D. C.

LABORATORIES, LANGLEY FIELD, VA.

Created by act of Congress approved March 3, 1915, for the supervision and direction of the scientific study of the problems of flight (U. S. Code, Title 50, Sec. 151). Its membership was increased to 15 by act approved March 2, 1929. The members are appointed by the President, and serve as such without compensation.

GEORGE W. LEWIS, *Director of Aeronautical Research* S. PAUL JOHNSTON, *Coordinator of Research*

JOHN F. VICTORY, *Secretary*

HENRY J. E. REID, *Engineer in Charge, Langley Memorial Aeronautical Laboratory, Langley Field, Va.*

JOHN J. IDE, *Technical Assistant in Europe, Paris, France*

TECHNICAL COMMITTEES

AERODYNAMICS
POWER PLANTS FOR AIRCRAFT
AIRCRAFT MATERIALS

AIRCRAFT STRUCTURES
AIRCRAFT ACCIDENTS
INVENTIONS AND DESIGNS

Coordination of Research Needs of Military and Civil Aviation

Preparation of Research Programs

Allocation of Problems

Prevention of Duplication

Consideration of Inventions

LANGLEY MEMORIAL AERONAUTICAL LABORATORY

LANGLEY FIELD, VA.

Unified conduct, for all agencies, of scientific research on the fundamental problems of flight.

OFFICE OF AERONAUTICAL INTELLIGENCE

WASHINGTON, D. C.

Collection, classification, compilation, and dissemination of scientific and technical information on aeronautics.

4-1-40

REPORT No. 682

FLAME SPEEDS AND ENERGY CONSIDERATIONS FOR EXPLOSIONS IN A SPHERICAL BOMB

By Ernest F. Fiock, Charles F. Marvin, Jr., Frank R. Caldwell, and Carl H. Roeder

SUMMARY

Simultaneous measurements have been made of the speed of flame and the rise in pressure during explosions of mixtures of carbon monoxide, normal heptane, iso-octane, and benzene in a 10-inch spherical bomb with central ignition. From these records, fundamental properties of the explosive mixtures, which are independent of the apparatus, have been computed. The transformation velocity, or speed at which flame advances into and transforms the explosive mixture, increases with both the temperature and the pressure of the unburned gas. The rise in pressure has been correlated with the mass of charge inflamed to show the course of the energy development.

Comparable mixtures of the three hydrocarbon fuels expanded about the same amount upon burning and therefore developed about the same power, despite differences in the rate of burning. The addition of ethyl fluid produced no measurable change in flame speed over the range of conditions studied. None of the characteristics of normal burning seems to give a clue as to the relative tendency of fuels to knock. The observed values of pressure are lower than these calculated on the assumption that reaction goes to equilbrium within a very short distance behind the flame front. This fact, together with other independent evidence points to a continued evolution of energy within gas that has already been traversed by flame.

INTRODUCTION

The practical objective of research on gaseous combustion, from the viewpoint of the automotive engineer, is the improvement of the combustion process as a source of power in engines. The character of the explosion greatly influences the power and efficiency and, to a considerable extent, affects smoothness of operation.

Although the modern internal-combustion engine has attained a high state of mechanical perfection, many important details of its combustion process remain obscure. Various means of controlling the explosion have been devised, but each improvement has increased the difficulty of further advance and emphasized the importance of a more exact knowledge of the fundamentals of the combustion process.

The spread of flame in an engine cylinder has been followed by various methods. The observed movements, however, result from the simultaneous operation of numerous factors that are not subject to independent control. Thus the engine, with its highly complicated combustion process, is poorly adapted to fundamental studies aimed at the isolation and precise evaluation of the separate effects of the operating variables. Recognizing this fact, the National Advisory Committee for Aeronautics has supported a continual investigation at the National Bureau of Standards to obtain such basic data for simpler types of explosions under carefully controlled conditions.

Some of the more immediate objectives of these studies are:

1. To provide additional information concerning the influence of the mass motion of the gases upon the velocity of the flame.
2. To develop facts that will help to evolve a clear, general picture, on a molecular scale, of the process of ignition and of the structure and the mode of propagation of flame.
3. To measure the transformation velocity, or the speed at which flame propagates into and transforms various explosive mixtures. This transformation velocity, as distinguished from the more readily observed speed at which flame moves in space, is a fundamental property of the mixture that determines the rate of pressure rise in an engine.
4. To evaluate certain indexes of the inherent energy of the explosive mixture, such as the expansion ratio and the rise in pressure per unit mass consumed.
5. To determine, if possible, the individual effects of charge composition, temperature, and pressure upon the burning characteristics of various fuels.
6. To search for possible relations among the normal burning characteristics of explosive mixtures, their physical and chemical properties, and their tendency to knock in an engine.
7. To obtain additional evidence as to the presence or absence of afterburning; that is, of continued evolution of energy in gases already traversed by the flame or, more exactly, the flame front.

8. To study the period just after ignition, during which the flame front has a positive acceleration.

Some of these objectives have been attained, either in whole or in part, in the studies herein reported; other of these objectives remain as subjects for future investigation.

Perhaps the simplest method yet devised (references 1 to 6) for studying explosions is one that makes use of a soap bubble blown with an explosive mixture and fired by a spark at its center. High-speed motion pictures of such explosions, which take place at constant pressure, show that a tiny sphere of flame originates at the spark gap and grows in radius at constant speed, retaining its spherical shape until all the mixture is inflamed. From photographic records showing the outward movement of the flame front, it is possible to compute an expansion ratio, namely, the ratio of the volume of the final ball of flame to that of the original bubble, and the transformation velocity or the fundamental speed of flame with respect to the explosive mixture.

Values of these characteristics have been obtained for a variety of simple gaseous mixtures, both with and without the addition of inert gases to the fuel-oxygen mixtures. (See references 1 to 7.)

The bubble, or constant-pressure, method has the great advantage that it requires neither the measurement of a rapidly changing pressure or of gas flow. It yields, however, only mean values of transformation velocity and expansion ratio for the entire explosion. Independent variation of the initial pressure, temperature, and concentration of water vapor within the bubble is impracticable. In addition, the method cannot be used for fuels such as hydrocarbons that dissolve in the soap film.

In order to extend the scope of the experiments, it seemed desirable to replace the soap film by a metal sphere, in which initial charge composition, temperature, and pressure could be controlled and varied over a much wider range than is possible with the bubble method. In such a constant-volume bomb, provision must be made for accurately and simultaneously recording both the spread of the spherical flame surface from the central spark gap and the resulting rise in pressure. From records of this kind, instantaneous values of several burning characteristics may be calculated at any desired stage in the explosion.

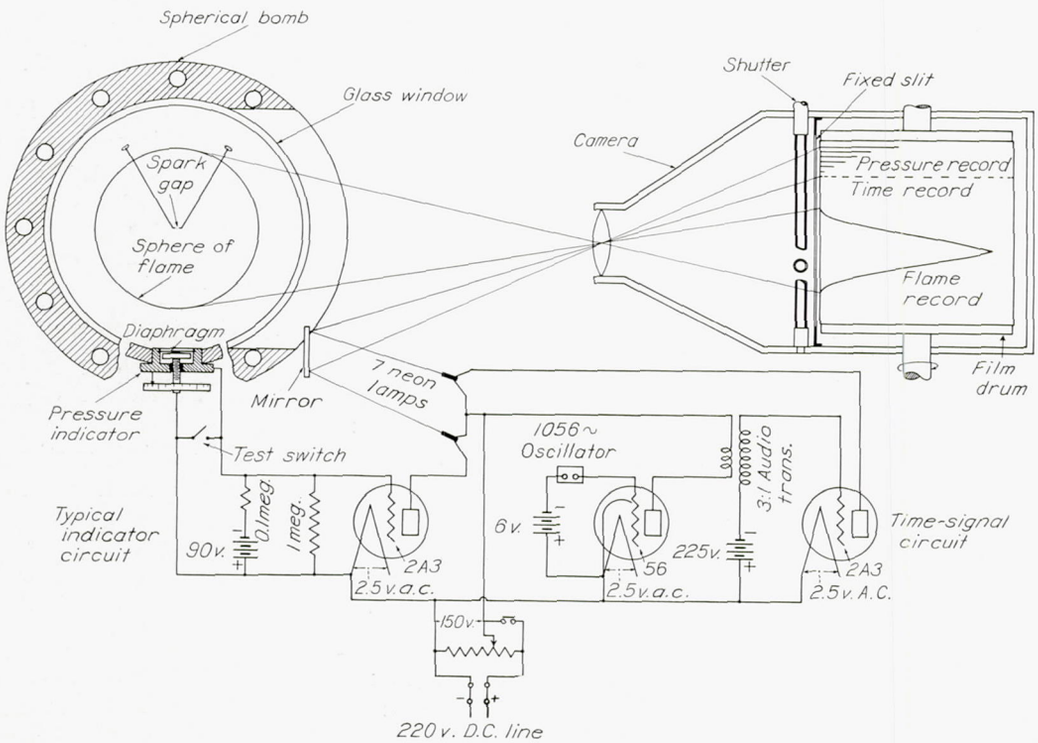

FIGURE 1.—Diagrammatic representation of apparatus.

This report describes the equipment and presents the results that have been obtained to date with such a bomb at the National Bureau of Standards.

APPARATUS

Briefly, the apparatus consists of a 10-inch spherical bomb with a central spark gap, a window through which the progress of the flame can be photographically recorded, and six indicators of the elastic-diaphragm type arranged to produce a record of the rise in pressure on the same film. The essential features are represented schematically in figure 1, which is largely self-explanatory and to which references will be made as the constituent parts of the equipment are individually described.

Spherical bomb.—Figure 2 is a photograph of the assembled bomb, rigidly supported on trunnions provided with leveling screws by means of which the narrow window is made vertical. The bomb itself consists of two identical spherical segments of stainless steel (internal radius, 12.243 cm.) between which the window assembly is clamped. The window, a short cylindrical ring of pyrex glass, is supported in recesses in two stainless-steel rings and sealed with hard wax.

The inner surface of the glass window is flush with the walls of the bomb, so that the combustion chamber is spherical, except for the ½-inch cylindrical element of glass. The supporting rings for the window are cut away in front to make the full vertical diameter of the bomb visible. Heavy bolts hold the parts of the bomb together, except in the region through which the flame is photographed, where a heavy clamp serves this purpose without obstructing the view of the flame.

Portions of the pressure indicators, to be described later, are shown in figure 2. The firing electrodes and the valves for introducing and withdrawing the gases are concealed at the rear of the bomb. The central spark gap is formed by two 0.5-millimeter tungsten wires, entering radially in the lower rear quadrant of the bomb.

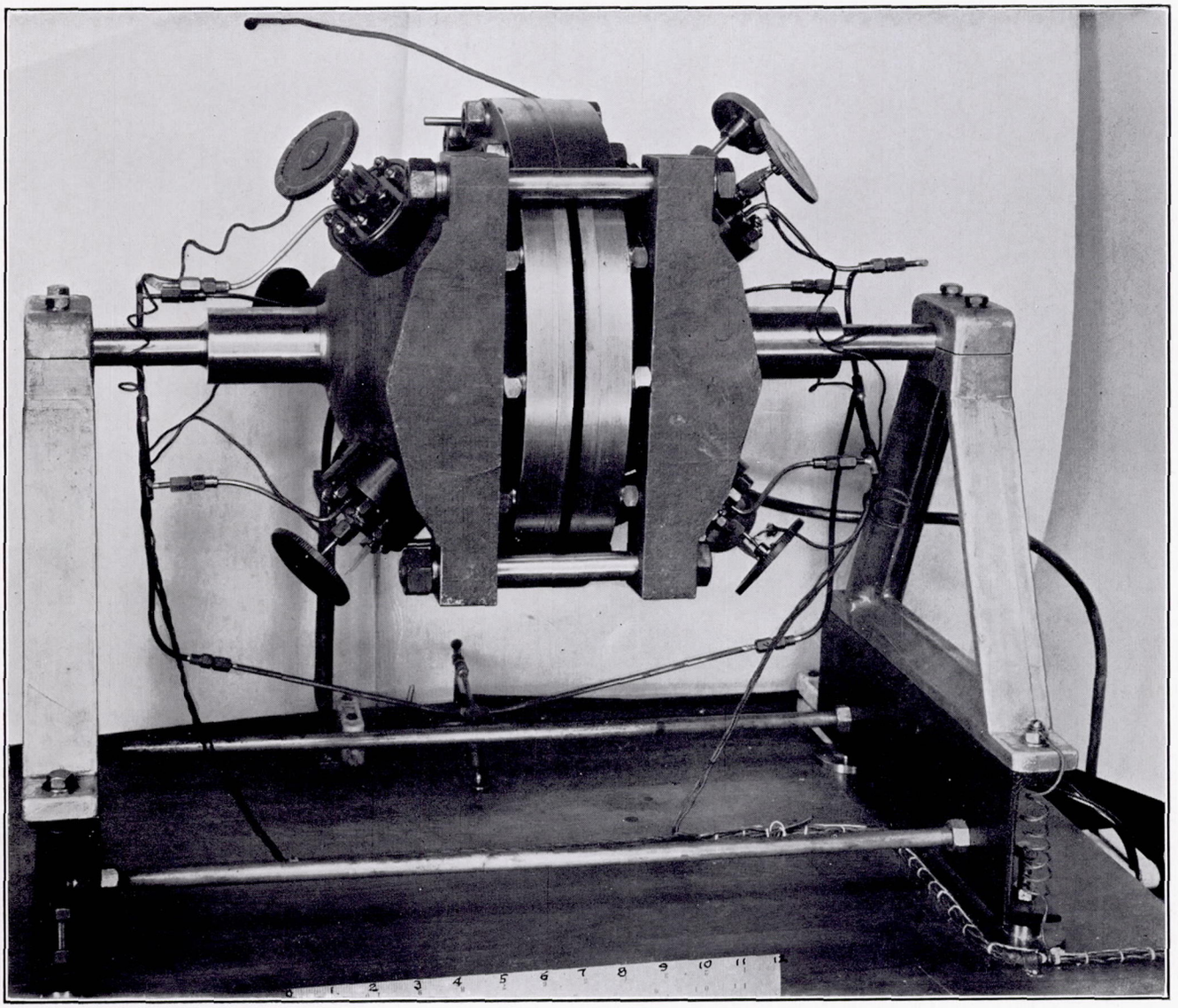

FIGURE 2.—The spherical bomb.

Camera.—Figure 3 is a general view of the apparatus, showing the bomb and its auxiliary equipment on one table and the camera on another. The essential features of the camera are shown diagrammatically in figure 1. A lens (F3.5; effective focal length, 7 inches) focuses the central plane of the bomb on a vertical element of a motor-driven drum carrying a 3⅞-inch by 12¾-inch film. As the drum revolves about its vertical axis, successive elements of the film are exposed to the light that comes through the narrow window of the bomb and produce a continuous record of the growth of the

sphere of flame. A fixed vertical slit, 0.08 inch wide, is placed as near the film as practicable to increase the sharpness and to control the timing of the image.

Just ahead of the fixed slit is a slotted tube, which rotates on a vertical axis to act as a shutter for the slit. This shutter, in effect, locates the image of the firing spark near the leading end of the film and limits the exposure to about four-fifths of a revolution of the drum. The mechanism for controlling the operation of the shutter is mounted on the cover plate of the camera, as shown in figure 4.

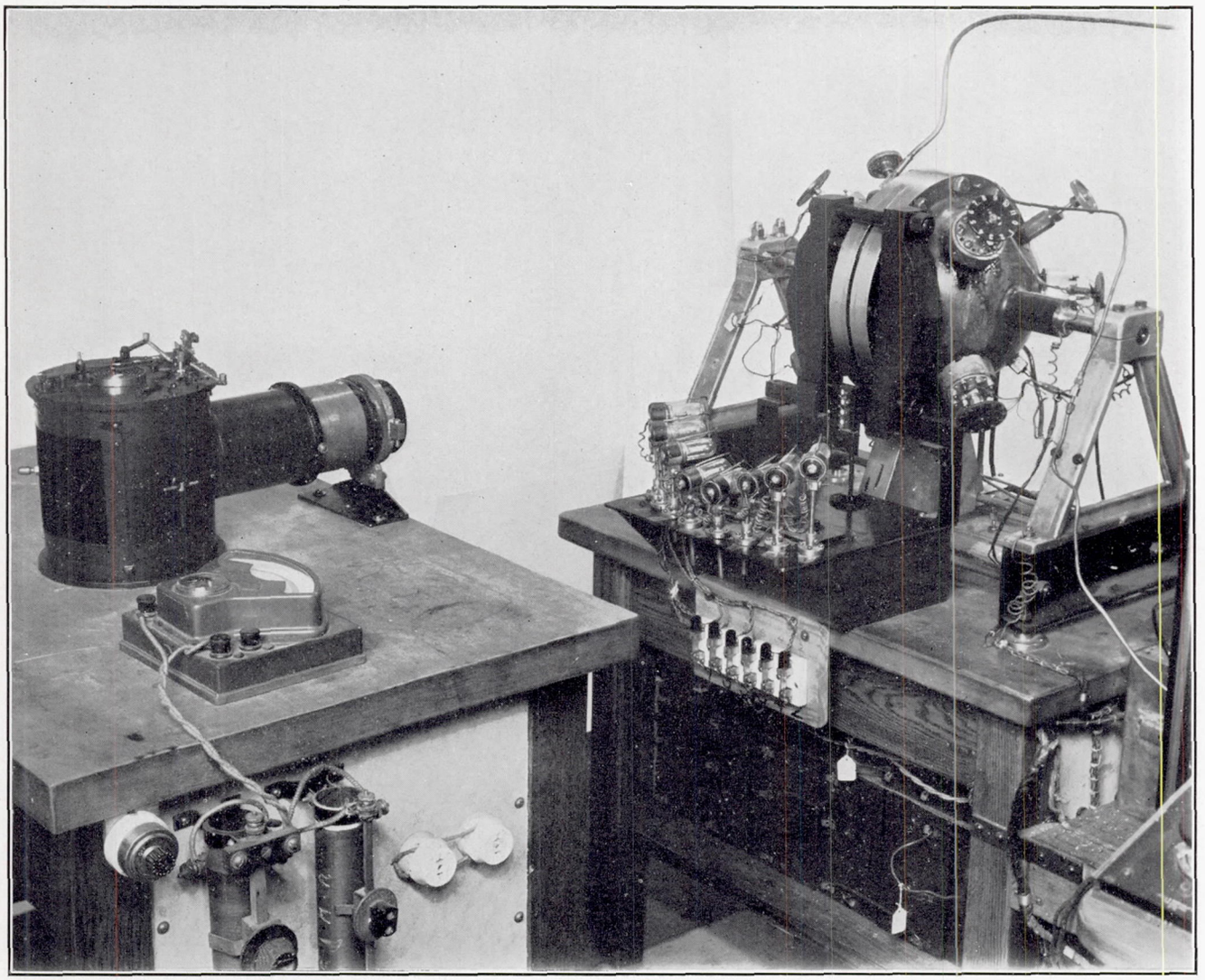

FIGURE 3.—General view of apparatus.

The coil springs C exert a couple tending at all times to rotate the shutter S in a clockwise direction. The times at which such rotation is permitted are fixed by an escapement lever E, the position of which is in turn determined by the position of a second lever L. This lever L is actuated by means of a pin P, which can be engaged in a spiral slot A in a disk rigidly attached to the film drum.

In operation, the shutter is initially placed in its limiting counterclockwise position (closed), the drum is brought to the desired constant speed, and catch D, holding lever L in an inoperative position, is manually released. A stiff leaf spring then suddenly shifts the lever L, engaging pin P in the spiral A, which thereafter synchronizes the position of the lever with that of the rotating drum. When the leading end of the film has just passed the fixed slit, the lever L has pushed the escapement lever E to such a position that the shutter will be quickly opened by the springs C. In this position, it is again stopped by the escapement lever, just as one of the shutter arms to which the springs are attached closes a contact that fires the charge in the bomb. Further movement of the lever L does not alter the position of the escapement lever until the trailing end of the film approaches the fixed slit. At this time, the end of lever L moves off the escapement lever, permitting a second clockwise rotation of the shutter to

the second closed position. The levers and the shutter are easily returned manually to the cocked position.

A flexible sliding door of spring steel in the rear of the camera case gives access to the drum, upon which the ends of the film are attached beneath inset metal strips held in their slots by screws. The use of supersensitive panchromatic film requires that the film be attached and removed in total darkness.

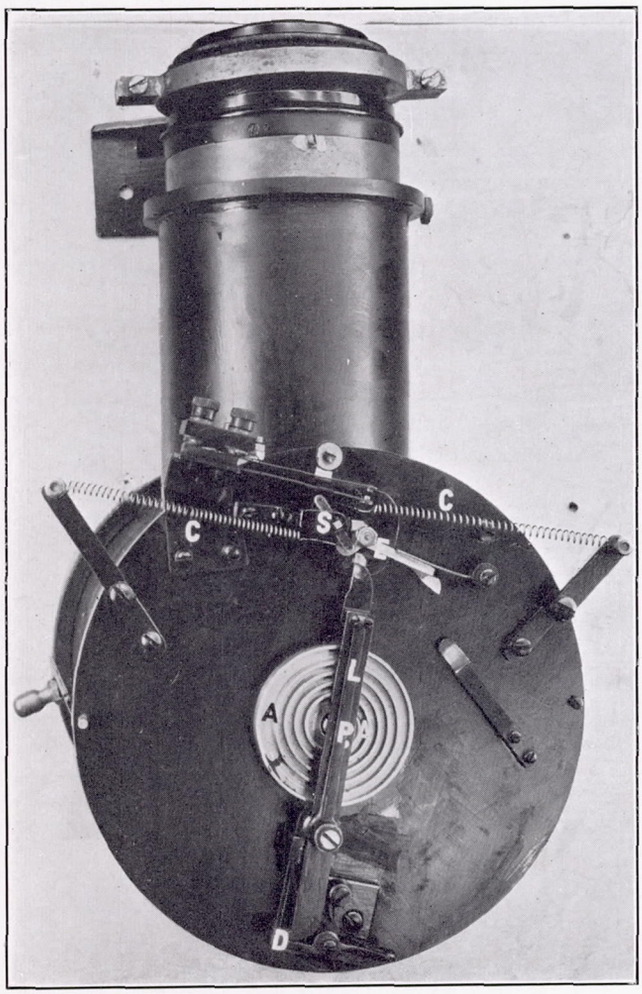

FIGURE 4.—Top view of camera.

The film drum is directly connected to the armature of a direct-current motor, the speed of which may be increased to approximately 4,200 r. p. m., corresponding to a film speed of about 73 feet per second. An electric tachometer is used to adjust the drum speed preliminary to firing.

Pressure indicators.—Since satisfactory results require high accuracy in the measurement of pressure, great care was taken in the development and the use of the pressure indicators. The diaphragm type of indicator was selected because of its inherent simplicity, adaptability, and high sensitivity. Test experiments showed that passages and backing disks could not be tolerated on the explosion side; the diaphragms were therefore mounted to form a part of the wall of the combusion chamber.

The details of an indicator are shown in figure 5. The spring-steel diaphragm D is clamped between the two brass body parts C_1 and C_2 through the right- and left-hand threaded band B. The electrode E is threaded (¼ inch, 48) through the lower part of the gland G and is sealed against leaks by paraffined leather packing P above the thread. Gland G, and hence also the electrode, is insulated from the rest of the indicator by the mica washers M and an air space. That part of the electrode above the packing is threaded to accommodate the lock nut N, which removes backlash, and the bakelite wheel W, which is graduated to provide for measurements of static sensitivity of the indicator. The stainless-steel contact F on the lower end of the electrode is slightly conical, with the vertex of the cone

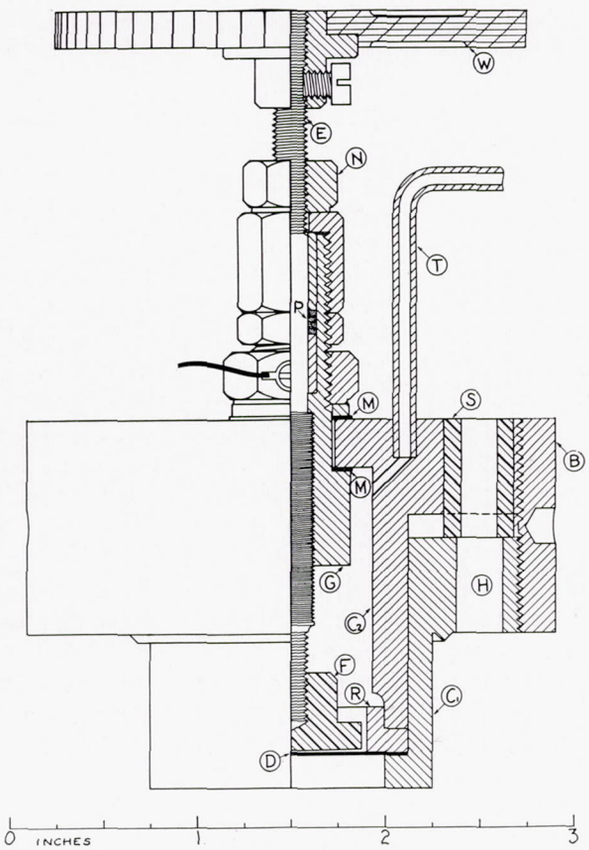

FIGURE 5.—Details of a pressure indicator.

toward the center of the diaphragm. This contact serves to support the diaphragm after the circuit is closed and to conduct heat away when the flame reaches the diaphragm. The ring R behind the diaphragm fixes the effective diameter, which in the experiments reported herein was in every case $1\frac{3}{16}$ inch. The pressure in the space behind the diaphragm, which may be controlled through tube T, was always made negligibly small by evacuation. All of the parts are made of brass, except those already specified.

Preliminary tests indicated that steel diaphragms 0.002 inch thick and $^{13}/_{16}$ inch in free diameter offered a satisfactory compromise between sensitivity and inertia effects, particularly when subjected to a high initial radial tension. In order to introduce this tension, the indicators, while loosely assembled without clamping the diaphragm, were cooled with dry ice. With the body of the indicator at this temperature and with a rod $^{13}/_{16}$ inch in diameter heated just above the melting point of tin (232° C.) held firmly against the diaphragm, the band was tightened and the hot diaphragm clamped in the cold brass. Upon returning to room temperature, the diaphragm cooled and shrank while its clamping rings warmed and expanded, leaving the diaphragm taut and flat. Some slipping of the steel relative to the brass is thought to have occurred, inasmuch as the sensitivities of the indicators were nearly alike after this treatment. Additional tension, with its consequent decrease in inertia error, was introduced by evacuating the space behind the diaphragms, thus introducing an initial deflection.

Each indicator is attached to the bomb by eight stud bolts, which pass through holes H in the indicator. By means of appropriate steel sleeves S, the force holding the indicator against the bomb is applied only to body part C_1. Distortions of other parts of the indicators are thus avoided. The seal to the bomb is made by placing a thin gasket of soft aluminum between a flat surface on the bomb and the V-shape bead on C_1.

Temperature control.—The pressure indicators, having taut steel diaphragms in brass mountings, were found to be quite sensitive to temperature. In order to minimize errors from this source, the room in which the bomb was used was provided with refrigeration and with automatically controlled compensating heaters. The initial temperature of the bomb in all the experiments herein reported did not vary by as much as 0.1° C. from 25° C. Such control effectively eliminated errors that might have arisen in its absence.

Measurement of static pressures.—All static pressures were measured with a mercury manometer. Recorded values of pressure are in terms of mercury at 0° C. and standard gravity.

Electrical circuit for indicators.—In order to produce a photographic record showing the exact instant at which the diaphragm of an indicator made contact with its insulated electrode, the arrangement shown in figure 1 was used. Briefly, contact between diaphragm and electrode removes the negative bias on the grid of vacuum tube 2A3 acting as a relay, permitting the plate current to flow through a crater-type neon lamp. This circuit was found to have a time lag of only 13 microseconds and, since but a very small current passes through the indicator contact, no difficulties with fouling or pitting of the contacts have been experienced.

Light from the neon lamp shines through a pinhole onto a mirror and is reflected into the camera lens which focuses it, through the shutter and fixed slit, to give a sharp line as the drum revolves. The origin of this line (see fig. 6), which is sharp and readily measurable, shows when the explosion pressure has reached the value for which the indicator was set.

Six similar indicators, each with its individual recording circuit, provide for the establishment of six points on the time-pressure curve for each explosion. Several explosions from indentical initial conditions are required to determine the entire pressure curve.

Time-signal system.—Time signals are recorded on each film by a seventh neon lamp, which is made to flash 1,056.7 times per second with driving equipment also shown in figure 1. The oscillations of a small tuning fork, driven by a 6-volt storage battery, are transformed into electric impulses by a tiny microphone. These impulses are amplified and then applied to the grid of a vacuum tube, the plate current of which lights the neon lamp in synchronism with the fork. The frequency of the fork was measured by comparison with the standard 1,000-cycle supply of the National Bureau of Standards and found to be independent of room temperature and driving voltage over the ranges which were experienced in service.

Magnification factor.—It being necessary to convert image size, as measured on the film, to actual size of the sphere of flame, the magnification factor of the lens system had to be determined. For this purpose, an accurate steel scale, placed vertically at the plane of the spark gap, was photographed through the window of the bomb. From this record, the ratio of image to object size was measured along the entire diameter of the bomb. The records having been photographed through the window, the corrections included any distortions due to imperfections in the glass. Additional correction was also made for the fact that the sphere of flame approached the camera lens as it grew in size.

PROCEDURE

Setting the indicators.—Prior to setting the pressure indicators, the temperature of the room and the bomb was brought to 25°C. Compressed air was then slowly admitted to the bomb until the pressure reached the highest value to be observed during the particular explosion. The electrode of an indicator was then adjusted to the position where contact with the diaphragm was just broken by tightening the lock nut N of figure 5. Admission of air was then continued very slowly until contact was remade, as indicated by the neon lamp. The pressure at which the lamp came on was read to the nearest 0.1 millimeter of mercury on a long mercury manometer, which could be used for all pressures up to 45 pounds per square inch absolute. The pressure in the bomb was then slowly decreased till the lamp went out and raised again as before, reading the pressure at the time of make. The process was repeated until several successive observations of pressure were

within ± 0.1 millimeter of mercury of the mean. The mean was taken as the pressure for which the indicator was set. The pressure in the bomb was then dropped to the next value selected for observation, a similar procedure was followed in setting the second indicator, and so on until all six had been set.

Preparation and introduction of explosive mixtures.—In all the mixtures studied, the oxygen was present in exactly the correct proportion for complete burning of the fuel. Each mixture of CO and O_2 contained 2.69 mole percent of H_2O, since data on this particular mixture were available from previous measurements (reference 7). The results include data for this CO mixture exploded at initial pressures of ⅓, ½, and 1 atmosphere and for dry mixtures of normal heptane, iso-octane (2, 2, 4 trimethyl pentane), and benzene with oxygen-enriched air, initially at a total pressure of 1 atmosphere.

The mixtures of CO, O_2, and H_2O were prepared in the bomb itself from pure, dry CO made by dehydration of formic acid, pure electrolytic oxygen, and distilled H_2O. The evacuated bomb was first connected to a small flask of water and an oil manometer. The water was admitted until its pressure, as indicated by the manometer, reached 2.69 percent of the total pressure which was to be attained. The CO and O_2 were then separately admitted until their partial pressures were 64.87 and 32.44 percent, respectively, of the contemplated total. At least 15 minutes were allowed for mixing before the charge was fired.

The mixtures of hydrocarbons with enriched air were prepared in a 25-gallon tank and withdrawn from this tank into the evacuated bomb. In order to prepare the mixture, the evacuated tank was connected to a receiver containing the liquid hydrocarbon and to a H_2SO_4 manometer. The hydrocarbon vapor was admitted to a previously selected pressure as indicated by the manometer. A mixture of N_2 and O_2 containing 36.7 percent O_2 was then admitted until the quantity of oxygen was chemically equivalent to the hydrocarbon present. The total pressure of the mixture was about two atmospheres in each case, so that six or seven successive runs from an initial pressure of one atmosphere could be made from one tank of mixture. After the gases were admitted to the 25-gallon tank, the mixture was allowed to stand for several days, during which time heat was applied at intervals to insure complete mixing. Explosive mixture was withdrawn from the tank into the evacuated bomb to the desired total pressure.

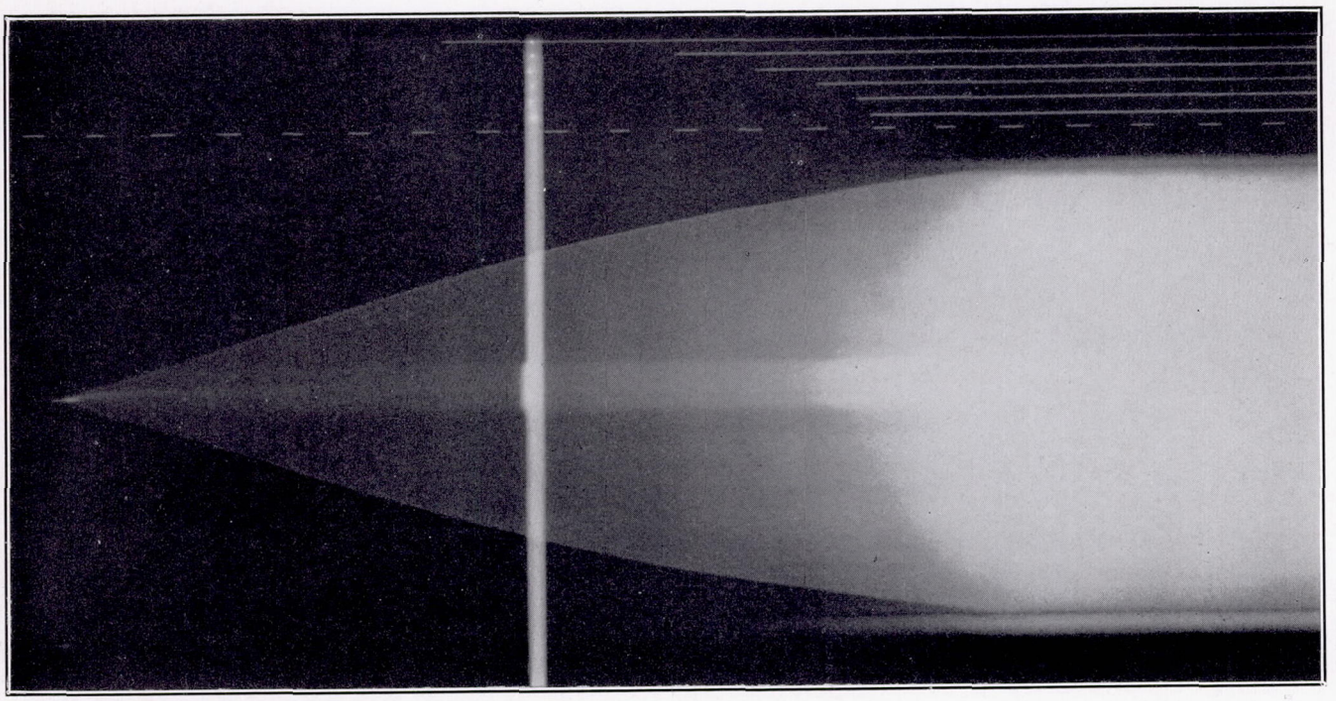

FIGURE 6.—Typical explosion record.

Typical explosion record.—Figure 6 is a full-scale reproduction of a typical explosion record, the fuel in this particular case being benzene. The entire travel of the flame is shown from the spark, seen at the apex of the symmetrical V-shaped trace, to the bomb wall. Some extraneous light leaves an image outside the bomb wall when the flame is nearly full size, probably owing to reflections from black surfaces as the angle of incidence approaches 90°.

Adjacent to the flame trace is the time record consisting of a series of uniform dashes of known frequency. Beyond are the six lines constituting the pressure record. Relative positions of the fixed slit, the firing spark, and the neon lamps were obtained by making

the exposures shown near the center of the record with the film stationary. Since the left edge of the slit should be in line with the firing spark for most accurate timing, a small portion of this edge was cut away in the neighborhood of the spark gap to insure that the spark would always appear in the picture. The greater width of the slit in this region accounts for the brighter streak down the center of the flame record. The electrodes at the spark gap photograph as a thin dark line, which serves as an axis of zero flame displacement.

The light streak extending across the figure is a still picture of the fixed slit in the camera, the neon lights of the pressure indicators, and the firing spark, made to permit the evaluation of small corrections for lack of alinement.

Measurement of the explosion records.—For purposes of measurement, each film was accurately alined on a piece of finely cross-ruled paper from which points on both upper and lower flame traces were read at convenient small intervals. Values of flame radius, twice read with the aid of a glass to the nearest 0.05 millimeter, were corrected for any distortion produced by the window and for the approach of the flame toward the lens. Readings thus corrected were multiplied by a previously determined magnification factor to yield actual values of flame radius. The distance from the firing spark to each measured value of radius was corrected for any misalinement of the firing spark and the timing edge of the slit and then was converted to its equivalent in time by multiplying by a factor determined from measurements of the dashed time record. A large-scale plot of flame radius in centimeters against time in milliseconds was then prepared. Generally there was close agreement between the two flame traces on a given record. Where any discrepancies existed, the curve was drawn best to represent all points. The flame traces thus obtained for the several explosions under identical conditions showed small variations but were, in most cases, practically parallel, indicating that the differences were principally in the very early stages, just after ignition. A mean time-radius curve for each initial state was finally prepared by averaging five or more individual flame traces.

The interval between the firing spark and the recording of each indicator was carefully measured on the films, corrected for any misalinement of the spark and the neon lamps as shown by the still pictures, and converted to milliseconds. Corresponding values of pressure and time for the several explosions at a given condition exhibited the same small variations as were found for the several flame traces. The relation between pressure and flame radius, however, was very consistent for all runs at a given initial condition, indicating that variations between runs were due largely to variations in flame speed, chiefly in the very early stages, rather than to variations in the volume of inflamed gas required to produce a given pressure rise.

The experimental data for a given initial state yield (1) a composite curve of flame radius against time obtained by averaging similar curves for from five to seven explosions under identical initial conditions, and (2) a set of from 30 to 42 corresponding values of pressure and flame radius for the same explosions. Pressure-time curves were obtained from the two relations previously described.

METHOD OF ANALYSIS

Equations by which the desired characteristics can be computed may be evolved if it is assumed that (1) the flame front is at all times a spherical surface; (2) compression of the unburned gas is adiabatic, that is, no radiation is absorbed and no heat is lost by conduction; (3) the gas mixtures obey the perfect gas laws, except that spectroscopic values of specific heat, which vary with temperature, are used; and (4) the pressure at any instant is uniform throughout the entire volume of the bomb. These assumptions are all reasonably correct, particularly for the first part of the explosion.

Symbols.—The symbols needed for the analysis and used throughout this report have the following significance:

R, radius of the spherical bomb (12.243 cm.).

k, ratio of specific heat at constant pressure to that at constant volume. The values of k used for the CO and hydrocarbon mixtures at 25° C. are 1.396 and 1.389, respectively.

The following symbols represent instantaneous values at time t:

p, total pressure.

r, radius of the sphere of flame.

M, mass of gas mixture.

V, volume.

D, density.

E, expansion ratio (ratio of the volume of inflamed gas at p to the volume of the same mass of unburned gas at p).

S_s, observed speed of flame in space $\left(\frac{dr}{dt}\right)$.

S_t, transformation velocity (velocity of flame relative to the unburned gas).

S_u, velocity of the unburned gas at the flame front $(S_s - S_t)$.

The instant of ignition is considered the reference zero of time. All properties of the gas mixture in its initial state are known and will be designated by the subscript 0, while those of the unburned and the burned portions of the charge are identified by the subscripts u and b, respectively.

Equations.—Suppose, as illustrated in figure 7, that the flame front has a radius r at time t. In the next increment of time dt, the flame front, advancing into the unburned gas at a velocity S_t, traverses a shell of thickness $S_t dt$. The total expansion occurring in time dt within the sphere of radius $r+S_t dt$ increases the total pressure by dp and forces the inner boundary of the remaining unburned gas outward to $r+dr$. Since the flame front moves a total distance dr in time dt, its instantaneous velocity in space is $S_s=\frac{dr}{dt}$.

During the inflammation of the shell of gas of thickness $S_t dt$, the remaining unburned gas undergoes an

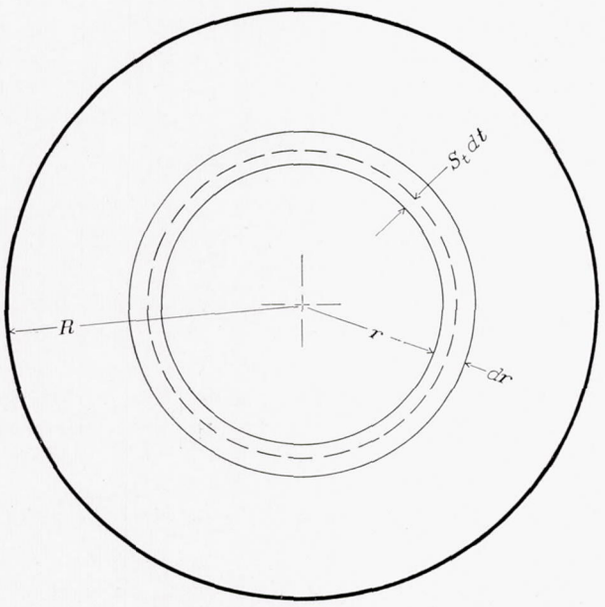

FIGURE 7.—Diagram for purposes of mathematical analysis.

adiabatic volume change of $-4\pi r^2(dr-S_t dt)$ in a total volume of $4/3\pi(R^3-r^3)$. Applying the adiabatic law in differential form to this compression,

$$\frac{dp}{p}=-\frac{k_u dV_u}{V_u}=\frac{3k_u r^2(dr-S_t dt)}{(R^3-r^3)} \tag{1}$$

Since $S_s=\frac{dr}{dt}$, equation (1) may be rewritten

$$\frac{S_s}{S_s-S_t}=\frac{3pk_u r^2}{(R^3-r^3)}\frac{dr}{dp}\equiv X \tag{2}$$

Values of k_u for the unburned mixture were calculated from available data on specific heats. Other quantities that appear in the definition of X in equation (2) may be obtained from the explosion records. Values of S_s and dr/dp are the slopes of the radius-time and the radius-pressure curves, respectively, and may be obtained either by graphical methods or through empirical formulations of the data.

From equation (2), it is evident that

$$S_t=\frac{(X-1)S_s}{X} \tag{3}$$

Values of the transformation velocity (S_t) calculated from equation (3) are the instantaneous rates at which the flame front advances into and transforms the unburned charge.

The total mass of gas within the flame front is

$$M_b=M_0-4/3\pi(R^3-r^3)D_u \tag{4}$$

in which D_u may be calculated from the adiabatic law

$$D_u=D_0\left(\frac{p}{p_0}\right)^{\frac{1}{k_u}} \tag{5}$$

The expansion ratio E at the prevailing pressure may be calculated by the equation

$$E=\frac{r^3}{R^3\left(\frac{p_0}{p}\right)^{\frac{1}{k_u}}-(R^3-r^3)} \tag{6}$$

ACCURACY OF THE OBSERVATIONS

Most of the important characteristics of the pressure indicators and the recording systems have been presented in previous sections. Preliminary experiments with diaphragms of different diameters and different thicknesses set to record the same pressure showed that, in spite of the differences in weight and amount of movement, the times of recording were very nearly the same. It is therefore believed that inertia lag does not introduce a serious error with any of the diaphragms tried, and particularly that the $^{13}/_{16}$-inch by 0.002-inch diaphragms under high initial tension provide a satisfactory compromise between sensitivity and inertia.

During each explosion, the diaphragms are subjected to two sources of heat; namely, direct conduction from the adjacent unburned gas and radiation from the flame. It is believed that the time intervals are too short to allow any appreciable heat flow by conduction during the first part of the burning, while there is not much change in the temperature of the unburned gas. As the flame approaches the walls of the bomb, however, the temperature of the remaining unburned gas increases more rapidly, and its effect upon the diaphragms may become appreciable. Therefore, the accuracy of the pressures measured during the very late stages of the burning may be somewhat decreased.

Heating of the diaphragms by radiation, like the heating by direct conduction, is very slight during the early stages of the burning. Possible effects of radiation were examined experimentally by polishing the inner surfaces of some diaphragms and painting others with optical black. With these indicators set to record the same pressure, the black diaphragms were fairly consistent in recording slightly earlier than the polished ones but, in general, the differences were no greater than

the accidental spread for identical indicators. Since the absorption of the blued diaphragms is nearer that of the polished than the black, it is believed that the radiant heat absorbed by the blued diaphragms was without significant effect upon the recorded pressures until very late in the burning process.

The flame speeds in the mixtures studied are so small compared with the velocity of sound that the calculated values of the pressure gradients existing in the bomb are within the limit of error of the actual pressure measurements. Furthermore, it is probable that the major portion of the gradient which does exist is confined to the neighborhood of the flame front.

It is impossible to assign an absolute value to the probable error in the values of pressure measured during an explosion, but no reason has been found for believing that the average individual observation differs from the true value by more than a few tenths of a millimeter of mercury. The portion of this error that is accidental, rather than systematic, should be at least partly eliminated by the smoothing operations applied in establishing the complete pressure relations.

The precautions and corrections applied in obtaining values of flame radius have been discussed in a previous section. Since the flame traces are continuous, an infinity of measurements of each trace is possible. Most of the error in measuring the films is eliminated by measuring the radius at a great many places on each record and subsequently plotting and smoothing on a scale about 20 times the image size. It seems reasonable that the smoothed values of flame radius are not in error by more than 0.2 millimeter and that the error rarely exceeds half this amount.

If, at any time, the flame trace ceases to be sharply defined or if any deviation from a truly spherical flame occurs, the errors in radius are larger by amounts that cannot be estimated. The appearance of such irregularities is subsequently discussed.

It is realized that some heat is lost by radiation from the inflamed gas and that some of it may be absorbed by the remaining unburned charge. The interior of the bomb being polished, most of this radiant energy is doubtless retained in the gases. The observed relations among pressure, radius, and time represent the actual state of the charge in the bomb, including possible effects of radiation. Its effects will therefore be reflected in the quantities derived from the observations. Data in the literature on radiation from the explosive mixtures studied are not adequate to yield reliable corrections at the present time. If, in the future, such data become available, the derived quantities may be recomputed. The best approximation for the present seems to be entirely to neglect the effects of radiation, until it is demonstrated that they are significant.

Careful study of the smoothed results indicates that the accidental errors may not greatly exceed 0.1 millimeter in r and 0.1 millimeter of mercury in p. Although no effort has been spared to reduce the systematic errors to these same limits, there is always a possibility that not all such sources of error have been eliminated. Even if the errors were actually within the just mentioned limits, they still constitute a restriction of the range over which desired characteristics may be derived from the measured quantities. This restriction results primarily from the fact that the volume (or mass) of gas that has been inflamed must be calculated. Any error in r is therefore multiplied by 3 when r is cubed to get volume. In addition, the mass inflamed during the early stages of the burning appears as a small difference between the large mass in the bomb and the comparably large mass of the unburned charge remaining.

The effects of assumed constant errors of 0.1 millimeter in r and 0.1 millimeter of mercury in p upon the

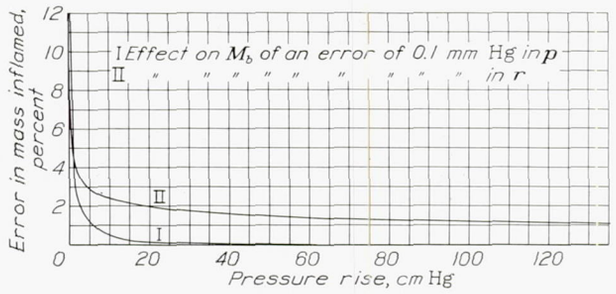

FIGURE 8.—Effects of assumed constant errors in pressure and radius upon calculated values of mass of charge inflamed.

calculated values of the mass of charge inflamed M_b for the case of $CO-O_2$ explosions from an initial pressure of one atmosphere are shown in figure 8. It is readily seen that, for very small values of pressure rise, the observed values of both p and r would have to be much more accurate than to the nearest 0.1 millimeter to permit the calculation of significant values of M_b. Thus it seems that at present there is little hope of obtaining sufficiently accurate measurements of either p or r to be useful during the earliest part of the explosion. For this reason, no attempt was made to measure values of pressure rise of less than 1.0 centimeter of mercury, at which condition the radius of the flame was about 4 centimeters.

Of all the possible sources of error that are known to the authors, only two would tend to make the observed value of pressure at any given value of flame radius too low. These sources are inertia lag in the diaphragm and time lag in the electrical circuits of the indicators. Experiments have shown that the effects of these two sources of error are negligibly small. It is therefore concluded that, for a given value of r, the observed value of p is more apt to be too high than too low.

EXPLOSIONS OF CARBON MONOXIDE AT VARIOUS INITIAL PRESSURES

During the development of the apparatus and the technique of securing and analyzing the observations, moist mixtures of CO and O_2 were used for several reasons. The individual constituents are easily prepared and handled in a very pure state and their mixtures in suitable proportions give a highly actinic flame that is readily photographed. In addition, previous measurements by the soap-bubble method furnished data for comparison that were available for no other fuel.

By the use of the apparatus and the procedure as finally developed, a series of careful measurements was

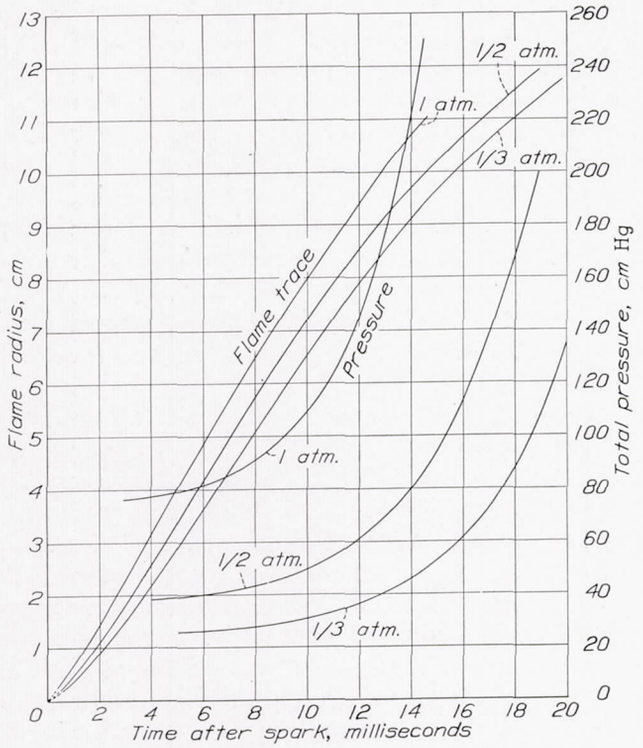

FIGURE 9.—Experimental data for CO at three initial pressures.

made with equivalent mixtures of CO and O_2 containing 2.69 percent of H_2O, fired at initial pressures of ⅓, ½, and 1 atmosphere. These results are presented in tables I and II, and time-radius and time-pressure curves, obtained by smoothing the experimental data as described under Procedure, are presented in figure 9. The analysis of these data illustrates the application of the method and reveals some interesting characteristics of the explosion process.

Flame speeds.—In figure 10, values of S_s, S_u, and S_t for an explosion of the CO mixture at one-third atmosphere initial pressure are plotted against flame radius. The data for one-half atmosphere initial pressure yield curves having similar characteristics.

At the beginning of the explosion, the transformation velocity is only a small fraction of the speed of flame in space. The major portion of S_s is the relatively high velocity S_u at which the flame front and the unburned charge just ahead are pushed forward by the expansion within the flame. This condition prevails only while the volume of the flame is small compared with the total volume of the bomb. As the burning progresses and the flame volume grows, the effect of new expansion in compressing the unburned charge outward decreases, while the amount of movement of the previously burned gas back toward the spark gap increases. The outward gas velocity is thus diminished, finally reaching zero at the bomb wall. At this point the flame advances in space through the last layer of gas at the transformation velocity.

During the burning, the temperature and the pressure of the unburned charge rise at an ever increasing rate owing to adiabatic compression. Figure 10 shows that the combined effects of these two operating conditions produce an increase in S_t.

It is obvious from the foregoing discussion that S_u, and hence S_s, are functions of the radii of both bomb and flame. Both are also dependent upon S_t because S_t determines the quantity of explosive mixture burned in unit time and thus the rate of outward motion due to

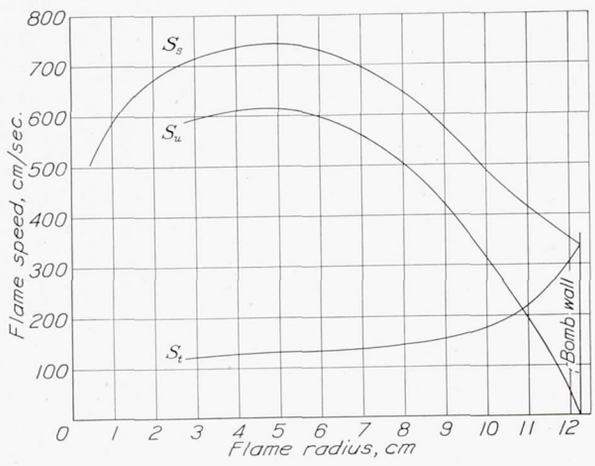

FIGURE 10.—Flame speeds for CO at one-third atmosphere.

expansion. In addition, S_u and S_s are affected by the amount of expansion per unit quantity of mixture inflamed. Thus, of the three velocities S_s, S_u, and S_t, only S_t is characteristic of the explosive mixture and independent of the configuration of the combustion chamber and the flame, except insofar as the chamber and the flame affect the conditions in the neighborhood of the reaction zone.

Inasmuch as the state of the unburned charge is practically uniform throughout the early stages of the burning, constant values of transformation velocity

and expansion ratio might reasonably be expected during this period. Such constant values of both S_t and E would result in decreasing values of S_s and S_u caused by growing values of flame radius. All the experimental values of S_s, for both CO and hydrocarbons, show, however, a marked increase during the first part of the explosion. It therefore follows that

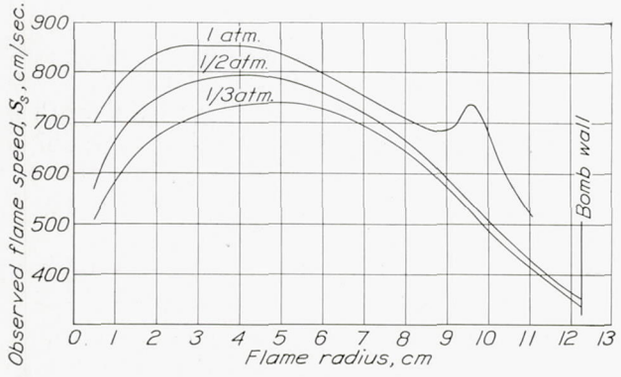

FIGURE 11.—Speeds of flame in space for CO at ⅓, ½, and 1 atmosphere

S_t or E, or both, must have values which, at the start, are abnormally low but increasing.

Unfortunately, the increasing values of S_s occur shortly after ignition, during that part of the burning for which, as illustrated in figure 8, a seemingly unattainable accuracy in the measurement of p and r is required for the evaluation of S_t and E. The factors that produce the initial acceleration must therefore be studied by some independent method.

In figure 11, the values of S_s for explosions of CO mixtures from initial pressures of ⅓, ½, and 1 atmosphere are shown. The initial increase in S_s becomes greater as the initial pressure is decreased, a fact previously observed (reference 8) during explosions in a glass bomb. Other experiments (references 8 and 9) have shown that the delay in attaining maximum flame speed is also increased as the concentration of water vapor in the CO mixtures is reduced.

A possible explanation of the delay period is that some time is required for the reaction zone to attain an equilibrium depth and structure. If the normal reaction zone does have a considerable depth, the flame front must travel at least this distance from the point of ignition before an equilibrium structure can be fully established. Previous to the attainment of the equilibrium state, both S_t and E may be abnormally low and increasing toward their normal values. If this explanation is correct, the depth of the reaction zone would appear to decrease as the pressure of the unburned charge is raised and as the concentration of water vapor is increased.

In figure 11, another abnormality in the movement of the flame appears in the form of a temporary increase in S_s in the neighborhood of $r=9$ centimeters for the explosion from an initial pressure of 1 atmosphere. Similar humps were always present in the curves for all explosions, both CO and hydrocarbons, from a pressure of 1 atmosphere, but none was ever found when the initial pressure was ½ or ⅓ atmosphere. In the general neighborhood of the hump, the photographic flame trace changes from a sharp, distinct edge to a somewhat blurred image. In some cases, the original trace not only becomes indistinct but is gradually replaced entirely by subsequent multiple traces. In figure 12, an explosion record having such a broken and multiple trace at point A, is shown. The effect is easily seen on the original negative but is more difficult to detect in the reproduction.

The deterioration of the sharp flame trace and the accompanying increase in S_s suggest a change in the structure of the reaction zone which increases S_t. An effect of this sort might result from a sudden change in the regime of burning, such as would occur if new reaction chains became predominant. Excitation of the unburned gas by radiation might have such an effect. Other possible causes are an unexpected departure of the flame front from a truly spherical shape or localized turbulence characteristic only of the apparatus. Interpretation of the experimental data beyond the point where the hump appears on the S_s curves at 1 atmosphere initial pressure must await further research to determine the nature of the disturbance.

In figure 13, instantaneous values of transformation velocity are plotted against total pressure for the CO explosions starting at ⅓, ½, and 1 atmosphere. The curves for ⅓ and ½ atmosphere are similar and appear reasonable, but that for 1 atmosphere reflects the hump in the S_s curve and therefore has a peculiar shape. Several isotherms have been drawn through points corresponding to equal temperatures in the unburned gas. A diagram of this sort would show at once the independent effects of charge temperature and pressure if these were the only operating variables affecting S_t.

Examination of the curves for the two lower pressures and the lower portion of the curve at one atmosphere reveals trends in S_t that are probably significant. There is a definite increase in S_t as the charge is compressed adiabatically. In general, the chart indicates also that S_t increases with pressure at any constant temperature, this effect being more noticeable at the higher temperatures and pressures. At any constant pressure, S_t shows a definite increase with temperature. Thus, there is evidence that transformation velocity is increased by a rise in either the pressure or the temperature of the unburned charge into which the flame is advancing.

It has been pointed out that flame speeds are abnormally low just after ignition and that, for the explosions starting at one atmosphere, there is a sudden and unexplained increase in flame speed at about 9 centimeters radius. Both of these effects probably involve

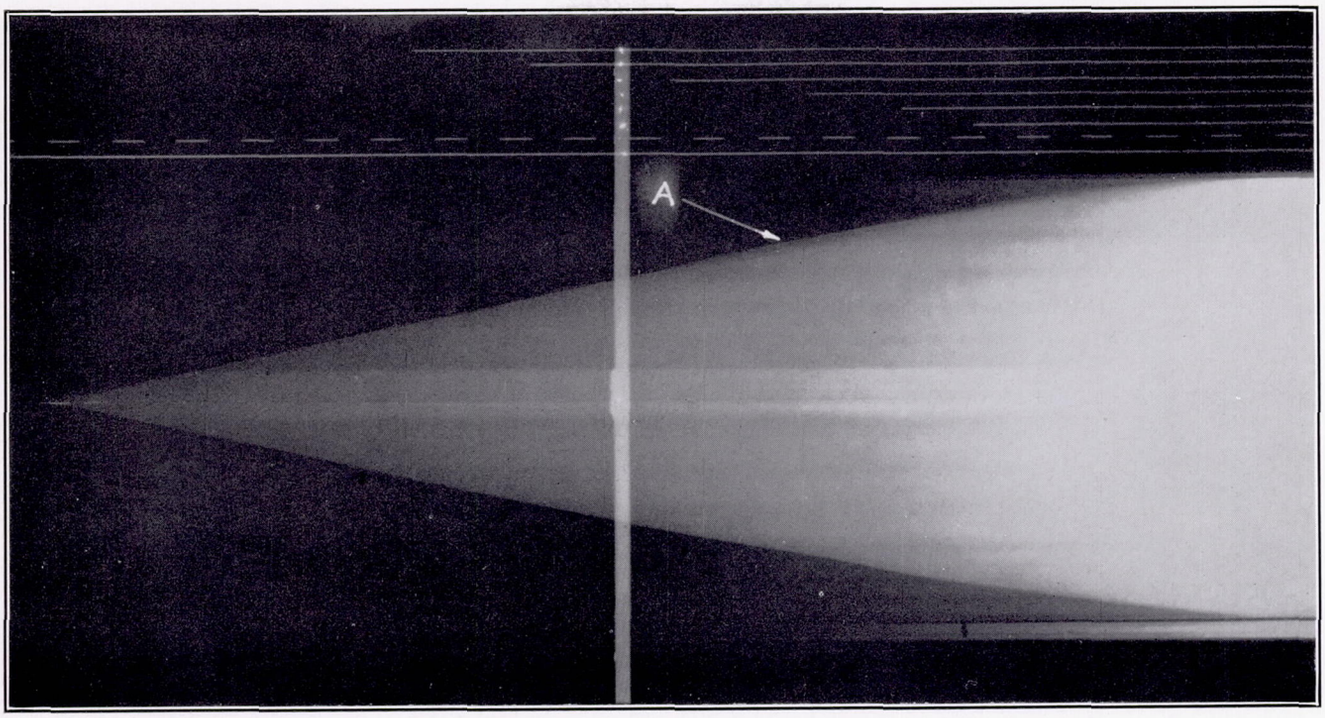

FIGURE 12.—Irregular flame trace, typical of explosions from one atmosphere.

changes in S_t that are not directly associated with the changes in temperature or pressure of the unburned gas but instead appear to be functions of what might be termed the "stage of the explosion." Thus, the stage of the explosion, as represented by the size of the flame, may, in effect, constitute a third variable, exerting an influence that cannot be isolated from the data presented in figure 13.

Energy relations.—The stage of the burning probably has more influence on the rate at which energy is developed during the explosion than on the transformation velocity because the pressure rise reflects the energy liberated throughout the entire volume of inflamed gas, while the transformation velocity is doubtless dependent only upon conditions in the near neighborhood of the flame front. The energy relations will now be treated independently of any considerations of flame speed.

The mass of gas within the sphere of flame at any time may be calculated from the radius-pressure relation by equation (4). In figure 14, the pressure rise is

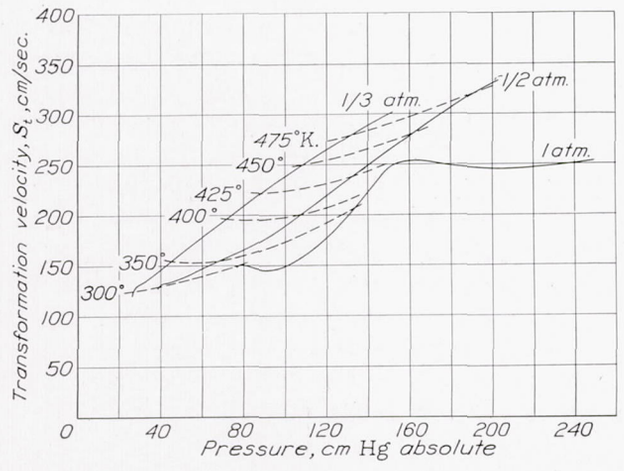

FIGURE 13.—Transformation velocity-pressure curves for CO at ⅓, ½, and 1 atmosphere.

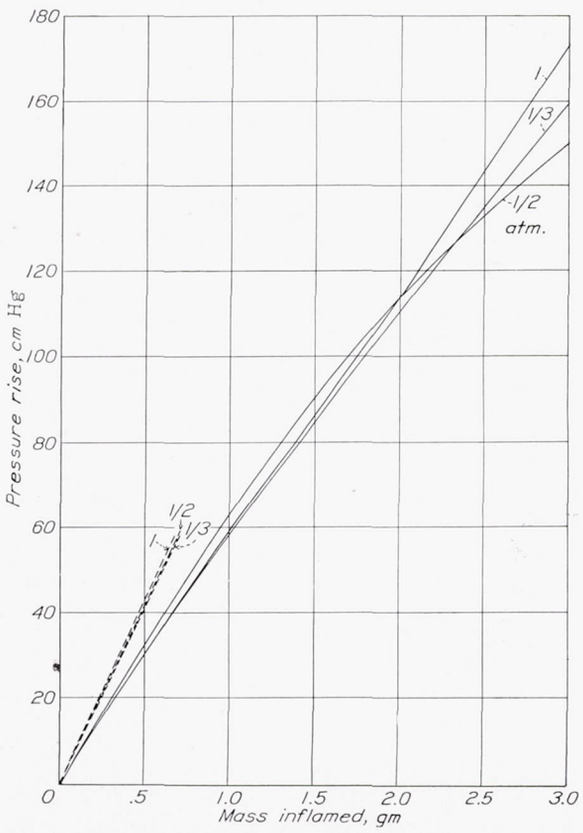

FIGURE 14.—Rise in pressure produced by inflammation of various masses of charge (CO at ⅓, ½, and 1 atmosphere).

plotted against the mass of gas inflamed for the CO explosions from the three initial pressures. It is evident that roughly the same rise in pressure results from the inflammation of a given mass of charge in each case. The small differences in the curves are believed to be of about the same magnitude as the experimental error, since the error is magnified by cubing the observed values of flame radius.

All three curves, however, have much smaller slopes than were expected. The three dashed lines in the lower left-hand corner of figure 14 have slopes that were calculated from purely thermal data for the early stages of the burning on the assumption that the chemical reaction goes to equilibrium in the flame front. The slope of the dashed line for one atmosphere is in good agreement with previous experimental results on the total expansion of an identical mixture fired at constant pressure in a soap bubble (reference 7).

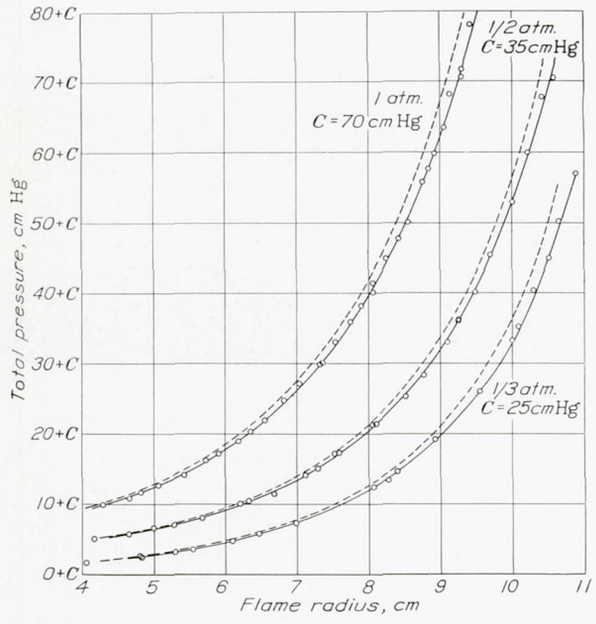

FIGURE 15.—Experimental and theoretical pressure-radius relations for CO at three initial pressures.

The differences between the theoretical (dashed) and the experimental (solid) pressure-radius relations are shown in figure 15 for the three series of explosions with CO. Similar differences were found later in studies with hydrocarbon fuels. (See fig. 22.) At every experimental point, the observed pressure is lower and the observed radius is higher than that calculated for complete burning in the flame front by an amount too great to be ascribed to experimental error, unless some systematic error has been completely overlooked. As previously pointed out, a thoroughgoing search has failed to reveal any error of this sort. Figure 15 further illustrates the relatively high precision of the experimental results.

The data, therefore, indicate that chemical equilibrium of the combustion products is not attained in a very thin flame front, as generally postulated in theories of normal burning. On the contrary, there seems to be a delayed reaction and heat liberation which persist within the inflamed gas for a considerable distance behind the flame front. This concept of a deep reaction zone, the thickness of which may vary with operating conditions, greatly complicates the interpretation of the results. Thus the slopes of the experimental curves of figure 14, which indicate the rate of pressure rise per unit mass of charge inflamed, reflect not only the energy liberated in the last increment of charge to enter the flame but also the energy released in a zone of unknown and perhaps changing depth.

A direct comparison of the energy relations as determined by the bomb and the bubble methods can be obtained by calculating the expansion ratio E for the early stages of the explosion in the bomb at one atmosphere initial pressure by means of equation (6). Such calculations show that E for the explosion in the bomb increases during the early stages and reaches a maximum of 6.2 when the flame radius is about .75 R. In the bubble experiments, the value $E=8.5$ was obtained for the over-all expansion of the same mixture. The theoretical value $E=8.3$ was calculated from thermal data on the assumption that the reaction goes to equilibrium in the flame front. The close agreement between the theoretical value of E and that for the bubble is to be expected, since the value for the bubble is based on the completely expanded sphere of flame and thus includes any expansion resulting from continued reaction after inflammation is complete. On the other hand, the values of E, calculated for a particular stage of the explosion in the bomb, do not include the energy which is latent within the inflamed gases and which is liberated later in the explosion. Thus, the low values of E that prevail during burning in the bomb may reasonably be attributed to the delayed liberation of energy in the flame and are therefore necessarily lower than the value obtained for the over-all expansion in the soap bubble.

In order to secure additional and independent evidence on the continued evolution of energy within the inflamed gases, sometimes termed "afterburning," observations of the gas movements within the sphere of flame were made by following the bright trails left by burning minute particles of black gunpowder that had been suspended in the mixture.

In this experiment, eight human hairs, more or less symmetrically spaced with respect to the spark gap, were stretched horizontally across the bomb. At the center of each hair, in the line of vision of the camera through the window, a few finely ground particles of powder were attached with very dilute shellac.

Figure 16 is a photograph of a $CO - O_2$ explosion from one atmosphere with such an arrangement inside the bomb. The hairs seem to offer no resistance to the motion of the flame, while the powder seems to ignite as soon as it is touched by flame and then to burn very brightly. It can be seen that the hot gases from the powder begin to move at once toward the center of the bomb. This movement continues for some time after the flame has reached the wall of the bomb, as indicated at point A in the photograph. The outward motion of the powder flame in the regions marked B is probably the result of contraction due to cooling at the wall.

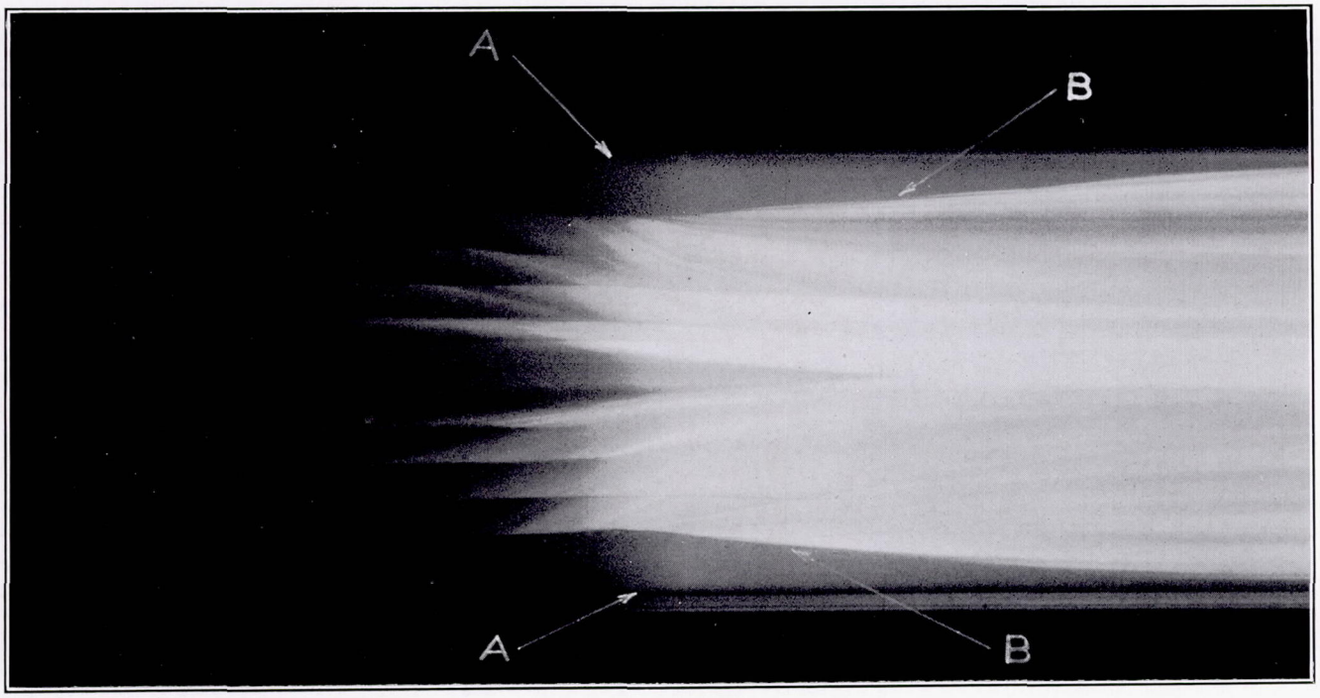

FIGURE 16.—Movements within the inflamed gas.

Two possible effects could cause the flame gases to move toward the center; namely, expansion in the gases that surround them and contraction in the gases that they enclose. Contraction in the enclosed gases could occur only if the gas near the center were losing heat by radiation at a seemingly improbable rate. It is therefore believed that the continued movement of the flame gases toward the center, after the flame hits the wall, indicates continued expansion in an outer shell of gas which has already been traversed by flame and that figure 16 is thus visible evidence of afterburning.

It is further believed that the inward movement of the central flame gas beyond point A cannot be due to burning of the powder because such small amounts were used and because the same movement of the flame gas was observed for each of a number of similar explosions where the powder was present at only one instead of eight points.

EXPLOSIONS OF NORMAL HEPTANE, ISO-OCTANE, AND BENZENE

At the completion of the studies with CO, a series of measurements with three hydrocarbon fuels was undertaken. The presentation of the results with these fuels follows the outline already used for CO, and many of the details need not be repeated.

For the survey of the burning characteristics of hydrocarbons, the reference fuels normal heptane (zero octane number) and iso-octane (100 octane number) were selected because of their similar chemical properties but widely different behavior in an engine under knocking conditions. Benzene, having a very different chemical structure, was chosen because of its relatively greater tendency to preignite than to knock. The comparative burning characteristics of these three fuels therefore seemed to be of considerable interest.

Preliminary experiments with the hydrocarbons showed that mixtures with pure oxygen burned too fast, whereas mixtures with air gave insufficient light for satisfactory photographic recording. Since only comparative results were sought, these difficulties were avoided by making the explosive mixtures with air somewhat enriched with O_2 (36.7 instead of 20.0 percent), the fuel and O_2 being always in chemically equivalent proportions. For all explosions in this series, the initial pressure was one atmosphere.

In a number of the figures that follow, the data already presented for the CO, O_2, H_2O mixture explod-

ing from one atmosphere are included to show the comparison of the burning characteristics for this radically different type of explosive mixture which evolves roughly the same energy as the hydrocarbon mixtures.

The basic experimental data for the three hydrocarbons and CO are presented in tables I and II and shown graphically in figure 17. Derived values of the speed of flame in space $\left(S_s = \frac{dr}{dt}\right)$ are plotted in figure 18. The differences among the four mixtures as represented in these figures are far greater than the experimental uncertainties. In general form, the spatial-velocity curves are quite similar, each showing the initial period of acceleration and the subsequent hump described in detail for the CO explosions.

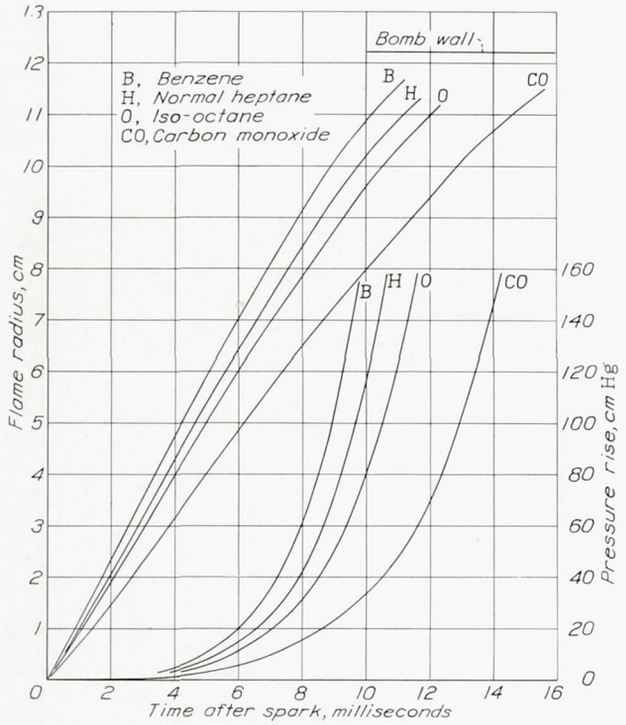

FIGURE 17.—Experimental data for benzene, normal heptane, and iso-octane.

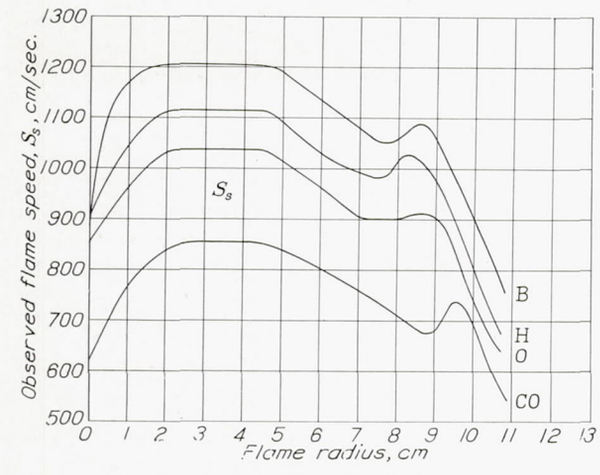

FIGURE 18.—Speed of flame in space for hydrocarbons.

Although the observed speed S_s is, in general, a function of the apparatus as well as of the mixture, the maximum values of S_s shown in figure 18 are essentially equal to the speed at which the flame travels outward from a point of ignition in free space. This condition is true because the maximum speed is attained before the walls of the bomb exert a significant influence on the expansion within the flame. Thus experiments with the CO mixture at atmospheric pressure yield a maximum value for S_s of 855 centimeters per second in the spherical bomb, as compared with previously measured values of 873 in a cylindrical bomb (reference 6) and 860 in soap bubbles (reference 7). The observed maximum values of S_s for the mixtures containing benzene, heptane, and octane are 1,204, 1,114, and 1,036 centimeters per second, respectively. The variation in S_s from fuel to fuel might result from differences in expansion upon burning or in transformation velocity, or both. It will be shown in the following figures that the transformation velocity is largely responsible for the observed differences in S_s.

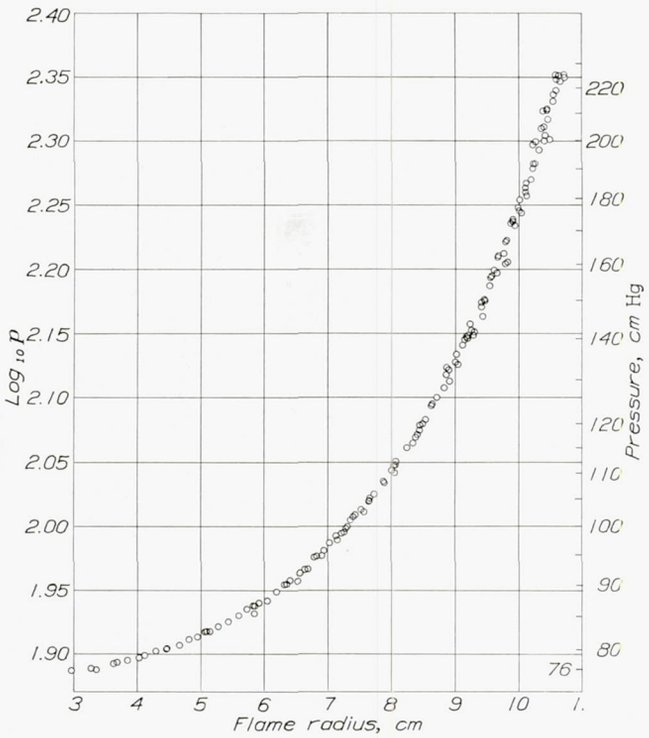

FIGURE 19.—Experimental pressure-radius relation for hydrocarbons.

For each experimentally determined pressure, a corresponding value of flame radius may be had from the explosion records. Every such point for all four fuels is shown in figure 19 on a logarithmic scale. Because of the large number of observations and the close similarity of the results for all the mixtures, the points for the various mixtures have not been sepa-

rately identified in this figure. The points for $CO–O_2$ are included, but it is accidental that they are so close to those for the mixtures of hydrocarbons with enriched air. This fact merely indicates approximate equivalence in the total energy liberated. It is clear from the figure that the expansion upon burning is about the same for all mixtures.

This result is exactly true, within the limits of experimental error, for the early stages of the burning of the hydrocarbon fuels. Here the experimental radius-pressure relation is the same for all three fuels, as is shown more clearly in figure 20, which also includes the curve of expansion ratio against pressure as calculated by equation (6) at a pressure of one atmosphere. During the later stages of the burning, small but consistent differences in expansion became apparent when

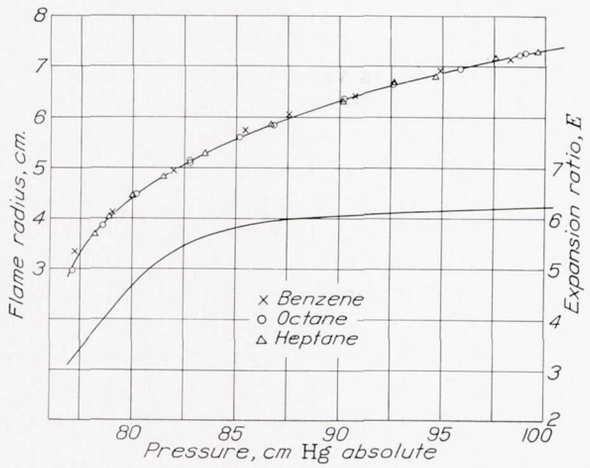

FIGURE 20.—Pressure-radius and pressure-expansion ratio relations for early stages of the burning of hydrocarbons.

the results for the separate fuels were individually treated, using either graphical or empirical algebraic formulations. The observed differences in S_s thus appear to be due principally to differences in S_t throughout the entire explosion and solely to this characteristic in the early stages.

Curves of transformation velocity S_t against pressure for the four fuels are shown in figure 21. As previously discussed for CO, these curves show a general trend toward higher values of S_t with increasing charge temperature and pressure and reflect the humps in the S_s curves. Efforts to explode the hydrocarbon mixtures at low initial pressures to obtain data for isolating the effects of temperature and pressure on S_t were unsuccessful because, in almost every trial, there was ignition both at the center and at the bomb wall where the spark jumped about one-half inch from the electrode to the ground.

The effect of the small differences in S_t, shown in figure 21, upon the speeds of flame in space can best be illustrated by the following numerical example. At $r=3.6$ centimeters and $p=78$ centimeters of mercury, the differences for benzene and octane are $\Delta S_s=170$ and $\Delta S_t=31.6$ centimeters per second. This ratio of about 5.4 applies also to the differences between benzene and heptane and between heptane and octane. It is thus apparent that transformation velocity has a very potent influence upon the speed at which flame moves in space through an explosive mixture.

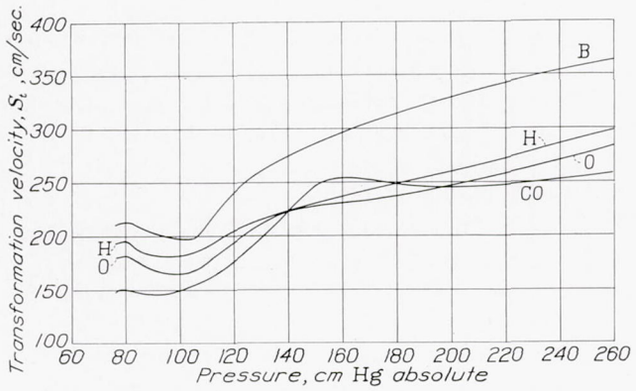

FIGURE 21.—Transformation velocities in hydrocarbon mixtures.

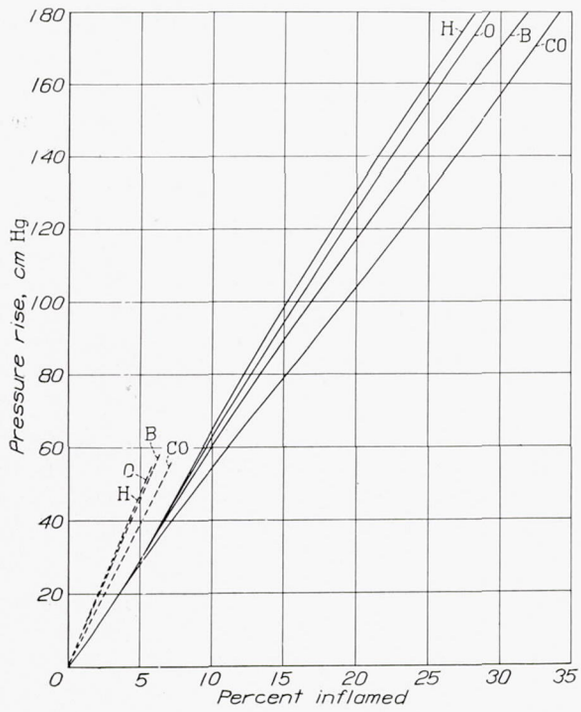

FIGURE 22.—Rise in pressure produced when various fractions of the hydrocarbon mixtures are inflamed.

In figure 22, the rise in pressure is plotted against the percentage of the charge that has been inflamed. The curves separate somewhat as the burning progresses. The dashed lines in the lower left-hand corner of this figure have the slopes that the experimental curves should have initially if the chemical reaction went to equilibrium in the flame front. The observed values of pressure are always lower than would be expected on the basis of this assumption. In this same connection,

values of expansion ratio shown in figure 20 are low at the start and increase to a maximum of about 6.2, which is considerably less than a theoretical value greater than 10 calculated by assuming that equilibrium is established in a negligible distance behind the flame front. Thus, again in the case of hydrocarbons, it appears that the actual reaction must continue for some distance within the flame, as was previously concluded in reference 10.

In figure 22, it will be noted that the experimental curves are in the same order as the thoeretical curves; that is, in the order of the ratios of hydrogen to carbon in the fuels. This order seems logical since the dissociation of CO_2 is several times as great as that of H_2O under the prevailing conditions.

In one experiment with normal-heptane, ethyl fluid, in an amount equivalent to 5 milliliters per gallon of liquid fuel, was added to the charge in the bomb. No measurable change in flame speed resulted. The deposit left on the interior of the bomb clouded the window so that it had to be cleaned. For this reason, the experiment was not repeated.

A thorough examination of all the characteristics of normal burning reveals that none can be correlated with the tendency of the fuels to knock. In fact, the relative behavior of all three fuels in the bomb is so nearly the same that high accuracy of the measurements is necessary to show any differences at all in those characteristics which are independent of the apparatus.

CONCLUSIONS

1. In all explosions that have been photographed, there is a short period just after ignition when the velocity of the flame in space is abnormally low and increasing. The duration of this period increases as the initial pressure is made less. The rise in pressure during the period of acceleration is too small to be measured with sufficient accuracy to show whether the low initial values of the speed of flame in space are due to subnormal values of transformation velocity S_t or of expansion E of the inflamed gas, or both. A possible explanation for this peculiarity of the explosion records is that some time may be required for the reaction zone to attain an equilibrium depth and structure and that the flame front must travel at least this far from the spark gap before a steady state can be established and before transformation velocity and expansion ratio can reach their normal values. If this theory is correct, the depth of the reaction zone appears to be greater at lower pressures.

2. Following the initial period of acceleration, the speed of flame in space reaches a maximum value that is practically constant until the walls of the explosion vessel begin to exert a significant influence on the outward motion of the flame. This maximum value is a complex property of the mixture, depending upon both S_t and E but independent of the apparatus when large containers with central ignition are used. Essentially the same maximum value for an equivalent mixture of CO and O_2 containing 2.69 percent of water has been observed with a spherical bomb, a cylindrical bomb, and with soap bubbles.

3. Carbon-monoxide explosions from initial pressures of ⅓ and ½ atmosphere show no unexpected irregularities in either the flame traces or the pressure records after the initial period of acceleration. Analysis shows clearly that, as the explosion progresses, the transformation velocity and the speed of flame in space approach equality, while the gas velocity component of the forward motion of the flame approaches zero at the bomb wall, in accordance with existing concepts as to the movements of flame and gases during an explosion.

4. In all the explosions at one atmosphere initial pressure, the flame trace becomes indefinite and the speed in space shows a sudden increase when the flame has traversed about three-fourths the radius of the bomb. Apparently, the structure of the reaction zone undergoes some change such as might result from the establishment of new reaction chains, from a departure of the flame front from a true sphere, or from local turbulence. Until further research indicates the nature and the causes of the disturbance, interpretation of the data must remain uncertain beyond the point where it occurs.

5. In all the explosions studied, there is a general increase in the transformation velocity as the temperature and pressure of the unburned charge rise because of the adiabatic compression.

6. In the explosions of CO and O_2, which it was possible to analyze for the independent effects of temperature and pressure, both of these variables appear to contribute to the increase in transformation velocity. Some uncertainty in the magnitudes of the effects arises from the possibility that other factors, associated in some obscure way with the stage of the burning, may influence transformation velocities to an unknown extent.

7. Transformation velocities are lowest for the CO explosions in spite of the fact that the CO was mixed with pure O_2 while the hydrocarbon mixtures contained large quantities of N_2.

8. For the hydrocarbons, the transformation velocity is highest for benzene and lowest for iso-octane, with normal heptane intermediate. Addition of ethyl fluid to the heptane mixture produced no appreciable change in flame speed. Thus there appears to be no relation between transformation velocity under the conditions of the experiments and the tendency to knock.

9. In explosions of CO and O_2, the pressure rise is approximately the same for a given mass of mixture inflamed, regardless of initial pressure. This result was expected from theoretical considerations, since the

only differences must result from rather secondary effects of temperature and pressure upon the chemical equilibrium.

10. During the early stages of the burning of the three hydrocarbons, there is likewise no measurable difference in the pressure rise produced when a given fraction of the charge is inflamed. Later in the burning, small differences do appear in the order of the hydrogen-carbon ratio of the fuels, as might be anticipated from the thermal properties of the products of combustion.

11. For all the explosions, the rise in pressure for a given mass of charge inflamed is considerably less than would be expected from calculations based on thermal data and the assumption that the chemical reaction goes to equilibrium in a very thin flame front. The results therefore indicate that the burning is not completed in a very shallow reaction zone but that reaction and heat liberation continue for some time after the flame front has passed.

12. Observations of the gas movements within the sphere of flame, made by following the bright trails left by burning particles of black gunpowder suspended in the mixture, also indicate the existence of continued reaction within the inflamed gases.

13. The experimental evidence indicating that the reaction zone has a considerable depth tends to confirm the explanation proposed in conclusion 1 for the early period of acceleration of the flame.

National Bureau of Standards,
Washington, D. C., *September 28, 1939.*

REFERENCES

1. Stevens, F. W.: A Constant Pressure Bomb. T. R. No. 176, N. A. C. A., 1923.
2. Stevens, F. W.: The Gaseous Explosive Reaction—The Effect of Inert Gases. T. R. No. 280, N. A. C. A., 1927.
3. Stevens, F. W.: The Gaseous Explosive Reaction—A Study of the Kinetics of Composite Fuels. T. R. No. 305, N. A. C. A., 1929.
4. Stevens, F. W.: The Gaseous Explosive Reaction at Constant Pressure—The Reaction Order and Reaction Rate. T. R. No. 337, N. A. C. A., 1929.
5. Stevens, F. W.: The Gaseous Explosive Reaction—The Effect of Pressure on the Rate of Propagation of the Reaction Zone and Upon the Rate of Molecular Transformation. T. R. No. 372, N. A. C. A., 1930.
6. Fiock, Ernest F., and Roeder, Carl H.: The Soap-Bubble Method of Studying the Combustion of Mixtures of CO and O_2. T. R. No. 532, N. A. C. A., 1935.
7. Fiock, Ernest F., and Roeder, Carl H.: Some Effects of Argon and Helium Upon Explosions of Carbon Monoxide and Oxygen. T. R. No. 553, N. A. C. A., 1936.
8. Fiock, Ernest F., and King, H. Kendall: The Effect of Water Vapor on Flame Velocity in Equivalent $CO-O_2$ Mixtures. T. R. No. 531, N. A. C. A., 1935.
9. Fiock, Ernest F., and Marvin, Charles F., Jr.: The Measurement of Flame Speeds. Chem. Rev., vol. 21, no. 3, Dec. 1937, pp. 367–387.
10. Rothrock, A. M., and Spencer, R. C.: A Photographic Study of Combustion and Knock in a Spark-Ignition Engine. T. R. No. 622, N. A. C. A., 1938.

TABLE I.—EXPERIMENTAL TIME-RADIUS RELATIONS

Mixture (mole percent) →	$CO=64.87$ $O_2=32.44$ $H_2O=2.69$			$C_6H_6=4.71$ $O_2=34.97$ $N_2=60.32$	$C_7H_{16}=3.23$ $O_2=35.51$ $N_2=61.26$	$C_8H_{18}=2.86$ $O_2=35.65$ $N_2=61.49$
Initial pressure → (atm.)	⅓	½	1	1	1	1
Time (millisec.)	Flame radius (cm.)					
0.5	0.158	0.201	0.322	0.529	0.466	0.433
1.0	.371	.464	.672	1.106	.974	.900
1.5	.628	.770	1.051	1.709	1.505	1.391
2.0	.912	1.103	1.449	2.304	2.051	1.898
2.5	1.209	1.456	1.865	2.908	2.609	2.415
3.0	1.523	1.817	2.286	3.510	3.164	2.933
3.5	1.847	2.191	2.714	4.112	3.720	3.451
4.0	2.181	2.578	3.141	4.713	4.278	3.972
4.5	2.524	2.967	3.569	5.308	4.835	4.489
5.0	2.876	3.361	3.995	5.888	5.379	5.005
5.5	3.235	3.758	4.425	6.451	5.905	5.511
6.0	3.598	4.153	4.849	6.998	6.411	5.998
6.5	3.965	4.552	5.268	7.528	6.916	6.476
7.0	4.331	4.947	5.678	8.055	7.409	6.936
7.5	4.702	5.341	6.078	8.594	7.896	7.384
8.0	5.073	5.727	6.476	9.125	8.409	7.835
8.5	5.443	6.105	6.863	9.625	8.913	8.286
9.0	5.814	6.484	7.235	10.082	9.386	8.742
9.5	6.178	6.854	7.608	10.504	9.824	9.192
10.0	6.535	7.215	7.970	10.890	10.215	9.614
10.5	6.886	7.568	8.317	11.240	10.571	9.997
11.0	7.228	7.908	8.664	11.561	10.900	10.349
11.5	7.566	8.240	9.035	----------	11.202	10.678
12.0	7.894	8.562	9.389	----------	----------	10.988
12.5	8.212	8.871	9.756	----------	----------	----------
13.0	8.520	9.166	10.101	----------	----------	----------
13.5	8.825	9.439	10.412	----------	----------	----------
14.0	9.117	9.705	10.700	----------	----------	----------
14.5	9.400	9.960	10.967	----------	----------	----------
15.0	9.668	10.203	11.225	----------	----------	----------
15.5	9.919	10.440	11.465	----------	----------	----------
16.0	10.155	10.672	11.705	----------	----------	----------
16.5	10.386	10.896	----------	----------	----------	----------
17.0	10.607	11.111	----------	----------	----------	----------
17.5	10.822	11.327	----------	----------	----------	----------
18.0	11.026	11.605	----------	----------	----------	----------
18.5	11.228	11.780	----------	----------	----------	----------
19.0	11.422	11.970	----------	----------	----------	----------
19.5	11.612	----------	----------	----------	----------	----------

TABLE II.—EXPERIMENTAL PRESSURE-RADIUS RELATIONS

Mixture mole → (percent)	CO=64.87 O_2=32.44 H_2O= 2.69						C_6H_6= 4.71 O_2=34.97 N_2=60.32		C_7H_{16}= 3.23 O_2=35.51 N_2=61.26		C_8H_{18}= 2.86 O_2=35.65 N_2=61.49	
Initial pressure → (atm.)	⅓		½		1		1		1		1	
Pressure (cm. Hg. abs.)	Radius (cm.)	Pressure (cm. Hg. abs.)	Radius (cm.)	Pressure (cm. Hg. abs.)	Radius (cm.)	Pressure (cm. Hg. abs.)	Radius (cm.)	Pressure (cm. Hg. abs.)	Radius (cm.)	Pressure (cm. Hg. abs.)	Radius (cm.)
26. 75	4. 060	40. 11	4. 165	77. 37	3. 275	77. 22	3. 335	78. 19	3. 685	77. 11	2. 960
27. 34	4. 530	40. 70	4. 650	78. 08	3. 630	79. 07	4. 120	78. 88	4. 030	78. 56	3. 850
27. 53	4. 830	41. 62	4. 970	79. 86	4. 295	82. 00	4. 945	80. 10	4. 460	80. 19	4. 470
27. 64	4. 815	42. 06	5. 285	80. 70	4. 665	85. 49	5. 745	81. 51	4. 817	82. 78	5. 140
28. 26	5. 290	45. 17	6. 205	81. 58	4. 815	87. 55	6. 050	83. 52	5. 275	82. 79	5. 095
28. 61	5. 550	45. 41	6. 330	82. 61	5. 060	90. 80	6. 410	86. 70	5. 855	85. 19	5. 600
29. 85	6. 100	46. 44	6. 685	84. 17	5. 435	94. 88	6. 915	90. 16	6. 320	86. 83	5. 840
30. 80	6. 470	49. 16	7. 125	86. 26	5. 735	98. 34	7. 140	92. 66	6. 690	90. 23	6. 360
32. 27	6. 970	50. 04	7. 300	87. 13	5. 920	101. 20	7. 370	94. 70	6. 800	92. 64	6. 655
37. 39	8. 077	52. 17	7. 535	88. 93	6. 200	102. 70	7. 580	97. 62	7. 163	95. 85	6. 950
39. 70	8. 400	52. 28	7. 595	90. 27	6. 360	104. 67	7. 655	99. 65	7. 295	98. 76	7. 225
44. 21	8. 935	56. 24	8. 050	90. 70	6. 530	108. 40	7. 895	102. 09	7. 440	99. 05	7. 270
51. 16	9. 550	56. 35	8. 105	91. 92	6. 560	112. 31	8. 080	104. 80	7. 670	101. 74	7. 410
58. 23	9. 980	60. 24	8. 510	94. 72	6. 820	115. 97	8. 350	110. 52	8. 020	105. 16	7. 670
60. 30	10. 095	63. 33	8. 765	97. 11	7. 040	120. 11	8. 500	117. 14	8. 397	111. 72	8. 080
65. 42	10. 295	68. 00	9. 095	99. 94	7. 320	124. 00	8. 640	119. 81	8. 460	118. 45	8. 420
69. 97	10. 525	71. 02	9. 250	100. 14	7. 355	128. 05	8. 840	124. 43	8. 650	118. 72	8. 455
75. 35	10. 655	71. 21	9. 255	103. 07	7. 535	131. 20	8. 875	132. 80	8. 980	125. 92	8. 730
82. 00	10. 885	75. 22	9. 480	105. 95	7. 745	132. 27	8. 915	139. 79	9. 167	134. 17	9. 020
84. 75	10. 930	80. 51	9. 700	108. 24	7. 900	136. 07	9. 040	143. 74	9. 255	140. 46	9. 200
88. 72	11. 020	80. 58	9. 700	110. 12	8. 060	140. 07	9. 200	149. 43	9. 430	140. 81	9. 225
93. 84	11. 180	88. 04	10. 000	111. 52	8. 060	142. 07	9. 275	156. 24	9. 570	150. 10	9. 475
99. 61	11. 250	88. 07	10. 020	114. 91	8. 250	145. 73	9. 450	162. 12	9. 680	156. 65	9. 595
106. 89	11. 410	95. 05	10. 215	117. 79	8. 420	149. 88	9. 480	172. 73	9. 917	162. 42	9. 685
114. 85	11. 535	102. 88	10. 415	120. 97	8. 550	153. 90	9. 560	179. 59	10. 025	166. 66	9. 805
119. 99	11. 615	106. 65	10. 575	125. 81	8. 755	157. 46	9. 675	185. 20	10. 125	172. 32	9. 885
129. 34	11. 730	117. 11	10. 780	127. 74	8. 840	158. 30	9. 630	193. 26	10. 240	173. 22	9. 915
139. 21	11. 845	117. 59	10. 730	129. 87	8. 930	163. 18	9. 780	204. 21	10. 360	177. 19	9. 995
149. 72	11. 975	120. 11	10. 790	133. 63	9. 060	167. 00	9. 820	211. 62	10. 456	183. 49	10. 110
.....	.....	127. 98	10. 930	138. 37	9. 135	171. 52	9. 945	225. 03	10. 590	191. 71	10. 235
.....	.....	134. 43	11. 085	140. 77	9. 300	176. 28	10. 015	.....	.....	199. 57	10. 280
.....	.....	142. 46	11. 160	141. 79	9. 310	182. 15	10. 115	.....	.....	204. 78	10. 410
.....	.....	149. 83	11. 315	148. 23	9. 430	186. 24	10. 200	.....	.....	210. 86	10. 400
.....	.....	149. 81	11. 290	160. 27	9. 800	190. 04	10. 230	.....	.....	210. 98	10. 455
.....	.....	150. 03	11. 260	160. 66	9. 835	191. 72	10. 265	.....	.....	217. 17	10. 545
.....	.....	.....	.....	175. 57	10. 050	196. 60	10. 335	.....	.....	223. 33	10. 605
.....	.....	.....	.....	180. 91	10. 135	201. 68	10. 425	.....	.....	.....	.....
.....	.....	.....	.....	199. 85	10. 420	207. 60	10. 470	.....	.....	.....	.....

U. S. GOVERNMENT PRINTING OFFICE: 1940

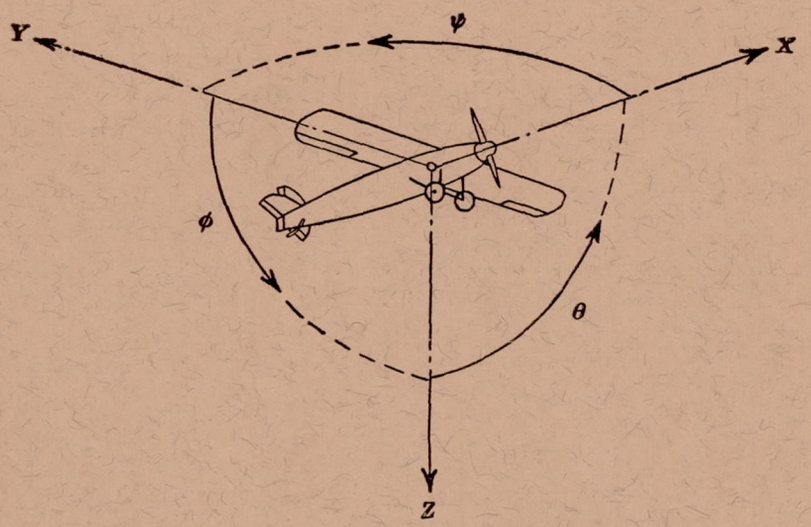

Positive directions of axes and angles (forces and moments) are shown by arrows

Axis		Force (parallel to axis) symbol	Moment about axis			Angle		Velocities	
Designation	Symbol		Designation	Symbol	Positive direction	Designation	Symbol	Linear (component along axis)	Angular
Longitudinal	X	X	Rolling	L	$Y \longrightarrow Z$	Roll	ϕ	u	p
Lateral	Y	Y	Pitching	M	$Z \longrightarrow X$	Pitch	θ	v	q
Normal	Z	Z	Yawing	N	$X \longrightarrow Y$	Yaw	ψ	w	r

Absolute coefficients of moment

$C_l = \frac{L}{qbS}$ (rolling) $\quad C_m = \frac{M}{qcS}$ (pitching) $\quad C_n = \frac{N}{qbS}$ (yawing)

Angle of set of control surface (relative to neutral position), δ. (Indicate surface by proper subscript.)

4. PROPELLER SYMBOLS

D, Diameter

p, Geometric pitch

p/D, Pitch ratio

V', Inflow velocity

V_s, Slipstream velocity

T, Thrust, absolute coefficient $C_T = \frac{T}{\rho n^2 D^4}$

Q, Torque, absolute coefficient $C_Q = \frac{Q}{\rho n^2 D^5}$

P, Power, absolute coefficient $C_P = \frac{P}{\rho n^3 D^5}$

C_s, Speed-power coefficient $= \sqrt[5]{\frac{\rho V^5}{P n^2}}$

η, Efficiency

n, Revolutions per second, r.p.s.

Φ, Effective helix angle $= \tan^{-1}\left(\frac{V}{2\pi r n}\right)$

5. NUMERICAL RELATIONS

1 hp.=76.04 kg-m/s=550 ft-lb./sec.

1 metric horsepower=1.0132 hp.

1 m.p.h.=0.4470 m.p.s.

1 m.p.s.=2.2369 m.p.h.

1 lb.=0.4536 kg.

1 kg=2.2046 lb.

1 mi.=1,609.35 m=5,280 ft.

1 m=3.2808 ft.